International Atomic Energy Agency

INDC(CCP)-275/L

INDC INTERNATIONAL NUCLEAR DATA COMMITTEE

TRANSLATION OF SELECTED PAPERS PUBLISHED IN NUCLEAR CONSTANTS 1, 1985

(Original report in Russian was distributed as INDC(CCP)-244/G)

Translated by the IAEA

June 1987

IAEA NUCLEAR DATA SECTION, WAGRAMERSTRASSE 5, A-1400 VIENNA

INDC(CCP)-275/L

TRANSLATION OF SELECTED PAPERS PUBLISHED

IN NUCLEAR CONSTANTS 1, 1985

(Original report in Russian was distributed as INDC(CCP)-244/G)

Translated by the IAEA

June 1987

Reproduced by the IAEA in Austria
June 1987

87-02612

Table of Contents

Experimental and Evaluated Data on Cross-Sections for (n,n'), (n,2n) and (n,3n) Reactions on ^{93}Nb 5
G.B. Kotel'nikov, G.N. Lovchikov, O.A. Sal'nikov, S.P. Simakov

Transmission Function Measurements, Evaluation of Mean Resonance Parameters and Group Constants for ^{235}U in the Unresolved Resonance Region 17
A.A. Van'kov, L.S. Gosteva, V.F. Ukraintsev, S. Toshkov, N. Yaneva

An Evaluation of the Spontaneous Fission Prompt Neutron Spectrum of ^{252}Cf 27
G.S. Bojkov, V.I. Yurevich

Angular and Energy Distributions of ^{252}Cf Spontaneous Fission Neutrons 53
E.A. Seregina, P.P. D'yachenko

EXPERIMENTAL AND EVALUATED DATA ON CROSS-SECTIONS FOR (n,n'), (n,2n) AND (n,3n) REACTIONS ON ^{93}Nb

G.B. Kotel'nikov, G.N. Lovchikov, O.A. Sal'nikov, S.P. Simakov

ABSTRACT

Compilation and analysis of the experimental data on cross-sections for the (n,n'), (n,2n) and (n,3n) reactions on ^{93}Nb have been carried out. Experimental results are compared with evaluated data from the INDL/V, ENDF/B-IV and ENDL libraries. It was concluded that experimental results are described most accurately by the INDL/V library data. Exceptions to this are cross-sections for the (n,2n) reaction and the high-energy part of neutron emission spectra, which, in the light of the most recent experiments, must be re-evaluated.

Wide practical use is made of niobium in reactor construction, and also in other spheres where nuclear physics is applied in technology and industry. It forms a part of many construction alloys used in nuclear installations, appreciably improving their mechanical and radiation properties. The existence of long-lived nuclear levels, excited in (n,n') and (n,2n) reactions, opens up the possibility of using niobium for dosimetric purposes. Niobium is of even greater interest as a material for future use in the construction of blankets for thermonuclear installations. Its high melting point, mechanical strength, large cross-section for the (n,2n) reaction and other properties are factors which make niobium a preferred material for limiting the high-temperature thermonuclear plasma zone.

Evidently, many aspects of the practical use of niobium are determined by the characteristics of the nuclear interaction between neutrons and this element, among which the inelastic scattering cross-sections and the (n,2n) reactions are of great significance. Taking into account practical needs, requirements have been formulated as to the accuracy of these characteristics: for the total cross-sections of (n,n') and (n,2n) reactions the figure is 5-20%; for the angular and energy distributions of reaction products it is 10-50% [1].

In order to satisfy these requirements experimental research is constantly being conducted, and evaluated data libraries are periodically revised. Neutron cross-sections for niobium are most fully represented in the following evaluated data libraries:

- The International Nuclear Data Library, INDL/V [3], which contains the evaluation carried out in 1977 by D. Hermsdorf and co-workers [2];
- The American national library ENDF/B-IV, compiled in 1974 [4] (in the fifth version of this library, which appeared in 1979, the data on the cross-sections under consideration for interaction between neutrons and niobium were not revised);
- The Evaluated Nuclear Data Library (ENDL) of the Lawrence Livermore National Laboratory, which was compiled in 1978 [5].

In the 5-10 years that have elapsed since these libraries were compiled, new experimental results have appeared. The authors of the present paper therefore made it their task to compare the evaluated and experimental data on the cross-sections for (n,n'), (n,2n) and (n,3n) reactions, with the aim of determining the degree of conformity between the data contained in the above-mentioned libraries and the new experimental data.

Neutron inelastic scattering cross-sections

Figure 1 shows experimental and evaluated data for the total neutron inelastic scattering cross-sections on niobium in the energy region from the reaction threshold to 20 MeV. There are three methods used for measuring the experimental data. In one of them, namely the reverse spherical geometry

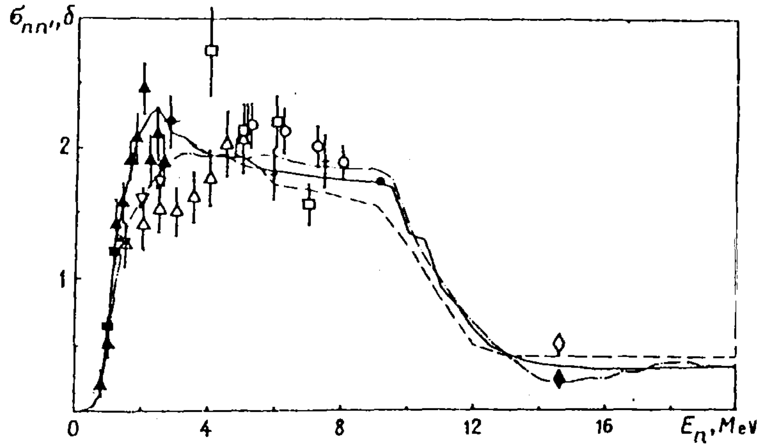

Fig. 1: Total cross-section of neutron inelastic scattering on ^{93}Nb

Experimental data: ▲ - [6]; ■ - [7]; ⊙ - [8]; ● - [9]; ▽ - [10]; □ - [11]; + - [12]; △ - [13]; ● - [14]; ○ - [15]; ♦ - [16]; ◊ - [17].
Evaluated data: —— - ENDL; - - - - ENDF/B-IV; —·—·— - INDL/V

method, neutrons scattered by a sample in the form of a hollow sphere are recorded by means of a ^{3}He ionization chamber. This integral method, which was used in the earliest experimental work [6, 7], contains considerable indeterminacies with regard to correct allowance for the background, multiple scattering in thick spheres and other factors. Experimental data obtained using this method may, therefore, contain significant systematic errors.

Another method consists in determining the neutron inelastic scattering cross-sections by means of measurements of the gamma quanta yield from the (n,n'γ) reaction [8-10, 18]. It is in such experiments that the best energy resolution is achieved, and this makes it possible to determine the partial neutron inelastic scattering cross-sections with the excitation of discrete energy levels. However, the energy range in which this method can be applied does not extend above 2-3 MeV, since with higher energies the spectrum of the gamma quanta being recorded becomes complex, and it is difficult to assess the population probabilities for a given nuclear level as a result of cascade transitions from the above-lying levels. As a rule, such indeterminacy leads to an over-evaluation of the inelastic scattering cross-sections at high incident neutron energies. The main body of experimental data [11-17, 19-21], including the results of the latest experiments [14-17], was obtained using the method in which the scattered neutrons are recorded according to their time-of-flight. While this method does not always ensure success in separating neutron groups which have been scattered with the excitation of discrete energy levels of the nucleus, it is nevertheless characterized by the high level of accuracy of the data obtained, since all methodological corrections are adequately taken into account.

It can be seen from Fig. 1 that, as a rule, the experimental data concur within the limits of the errors ascribed to them by the authors. Exceptions to this are the data in Refs [6, 9] for a neutron energy of approximately 2 MeV, and those in Ref. [11] where the energy is 4 MeV. As pointed out above, the peculiarities of the reverse spherical geometry method used in Ref. [6] and the complexity involved in deconvoluting the gamma-spectra [9] probably led to the fact that the data contained in these references contain systematic errors. If these points are not taken into account, then the average spread of the experimental data will be approximately $\pm$ 10%.

In the neutron energy region lying above the (n,2n) reaction threshold, equal to 8.92 MeV, the cross-section for the (n,n') reaction begins to diminsh sharply. The experimental data in this region are limited by an initial energy of 14.6 MeV [16, 17]. However, the cross-section evaluations obtained in these references should be considered approximate, owing to the indeterminacies arising from the isolation of the spectrum of the first neutron [16] and to the complexity of direct measurements of neutrons from the (n,n') reaction on the basis of coincidence with the accompanying gamma quanta [17].

As regards evaluated data, it can be seen from Fig. 1 that the best description of the experimental cross-sections is provided by INDL/V. Taking into account that the accuracy of these evaluated data is 20% [2], it may be considered that INDL/V satisfactorily describes the entire body of known experimental results. It would appear that the evaluated data provided by ENDF/B-IV and ENDL in the 1-3 MeV energy range give excessively high cross-sections.

In relation to the partial excitation cross-sections of discrete groups of energy levels (Fig. 2) there exists a fairly large body of experimental

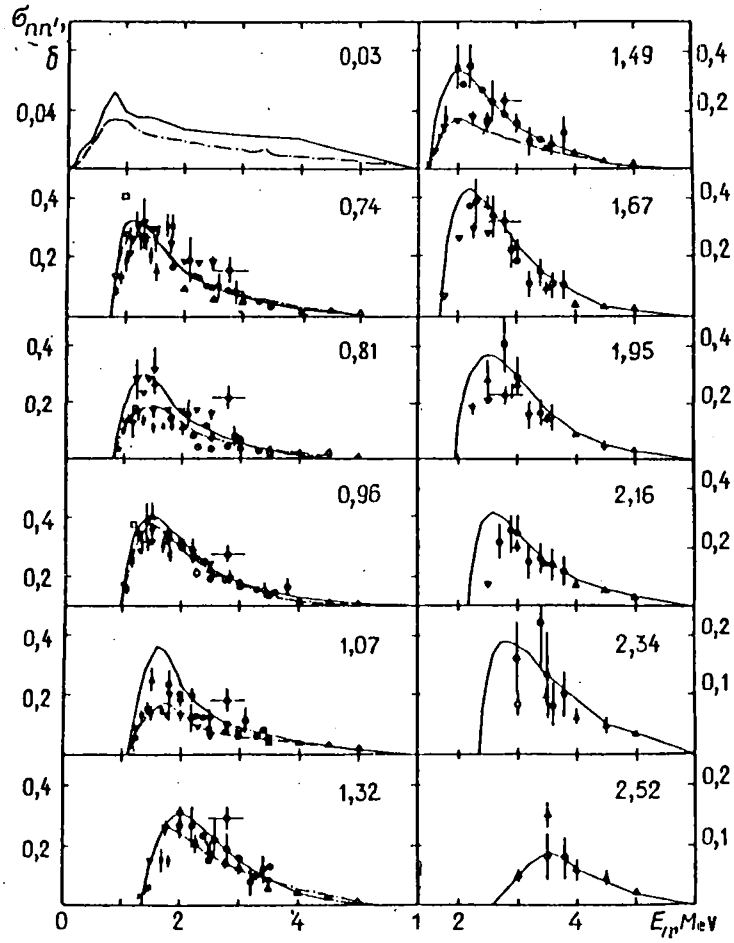

Fig. 2: Partial cross-sections of neutron inelastic scatering on ^{93}Nb (the energies of excited groups of energy levels in MeV units are shown in figures).

Experimental data : o – [9]; × – [18]; ▽ – [10]; ▼ – [19]; △ – [13]; ● – [20]; ○ – [21]. Evaluated data : — ENDL; – – – – ENDF/B-IV; —·— – INDL/V

data from different authors [9, 10, 13, 18-21]. As a rule, there is satisfactory agreement between them. The overall energy dependence of the cross-sections, as in the case of the total cross-section for the (n,n') reaction gives rise to the data in Ref. [9]. This points to the presence within these data of systematic errors. In the case of a group of energy levels with an average excitation energy of 1.49 MeV, an appreciable stratification of the experimental data is observed. Smaller cross-sectional values are obtained in experiments carried out using the gamma-quanta recording method [10, 18], while larger values are obtained from the neutron time-of-flight method [13, 21]. It would appear that, owing to the poorer energy resolution, the data in Refs. [13, 21] receive a contribution from the nearby energy levels. The comparison made between evaluated and experimental data in Fig. 2 shows that the evaluated data from INDL/V provide a better description of the experimental results.

Cross-sections for (n,2n) and (n,3n) reactions

A comparison of experimental and evaluated data for the integral cross-sections of (n,2n) and (n,3n) reactions on ^{93}Nb is set out in Figs. 3a and 3b respectively. The majority of experimental data is obtained by means of the simultaneous secondary neutron recording method, involving use of a large scintillation tank [22-26, 28]. Some of the data are determined by means of isolating the spectrum of the second neutron from the experimental spectra of the emission neutrons, measured by the time-of-flight method [16, 27]. As can be seen from Fig. 3a, the experimental data agree with each other within the limits of error. The evaluated cross-sectional values for the (n,2n) reaction deviate significantly from the experimental data in the neutron energy range above 15-17 MeV, and also lie systematically higher than the data which appeared later [26]. For a better description of the cross-section for the reaction ^{93}Nb(n,2n) we can recommend the evaluated data obtained by the authors of Refs. [29] or [30].

As regards the cross-section for the (n,3n) reaction, the data from Ref. [25], in which they are measured up to an energy of 24 MeV, are now well known. As is shown by Fig. 3b, the figures from the ENDL evaluation are a

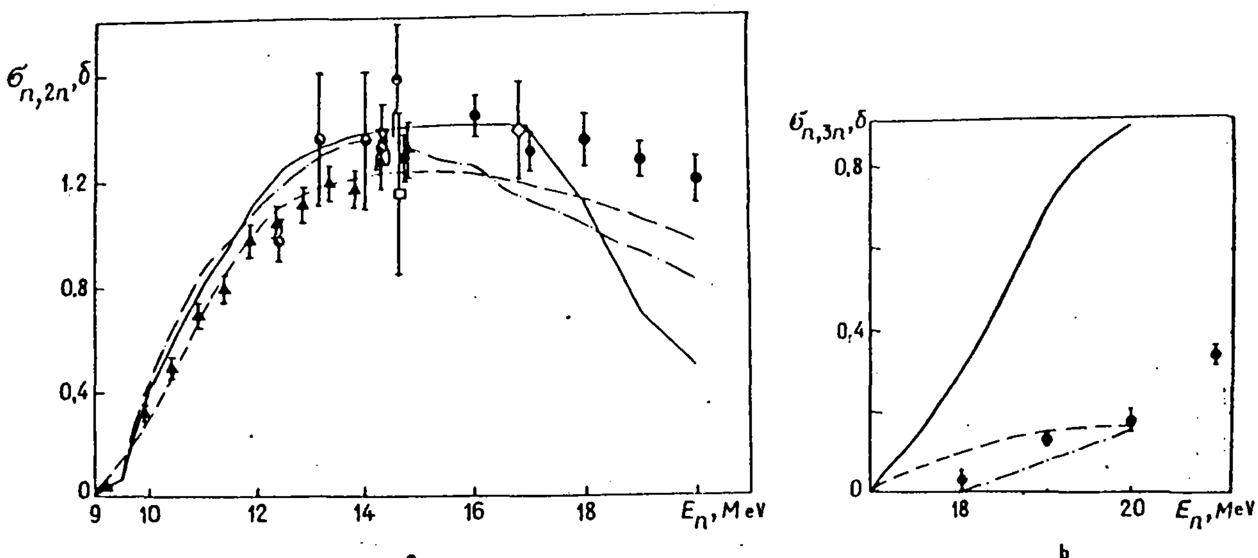

Fig. 3. Cross-sections for reactions: a – ^{93}Nb(n,2n) ; b – ^{93}Nb(n,3n). Experimental data : ◊ – [22]; ○ – [23]; ⊙ – [24]; ● – [25]; ▲ – [26]; □ – [27]; ⊖ – [28]; ▽ – [16]. Evaluated data : —— – ENDL; – – – – ENDF/B-IV; —·— – INDL/V

good deal too high, whereas the quality of the description given by the ENDF/B-IV and INDL evaluations is almost identical.

Emission neutron spectra from (n,n'), and (n,2n) and (n,3n) reactions

In recent years the attention of a large number of experimentalists and theoreticians has been attracted by emission neutron spectra. This is connected with the fact that the energy and angular distributions of the neutrons - the reaction products - provide a wealth of information about the nuclear interaction mechanism and the structure of excited states in atomic nuclei. In the light of recent experimtal research it has been possible to widen considerably the energy range and to refine the accuracy of measured cross-sections for niobium. New data has become available for the 5-8 MeV energy range [15]; experiments conducted at an energy level of about 14 MeV [31-35] have added greatly to the results previously obtained for this energy level [36-38]; the first measurements at energy levels of 21 MeV [39, 40] and 26 MeV [41] have been carried out. A comparison between these experimental data and the evaluated data is given in Figs. 4 and 5.

It should be noted that the angular secondary neutron distributions contained in all evaluated data libraries are isotopic in character. However, experimental data reveal an angular anisotropy: a symmetrical (relative to a 90° angle) distribution in the low-energy part of the secondary neutron spectra and a strong forward directionality in the high-energy part. As can

Fig. 4: Integral spectrum of neutron inelastic scattering with an initial energy of 6.2 MeV:

O - Experimental data [15]. Evaluated data -
——- ENDL ; - - - - ENDF/B-IV; —·— - INDL/V

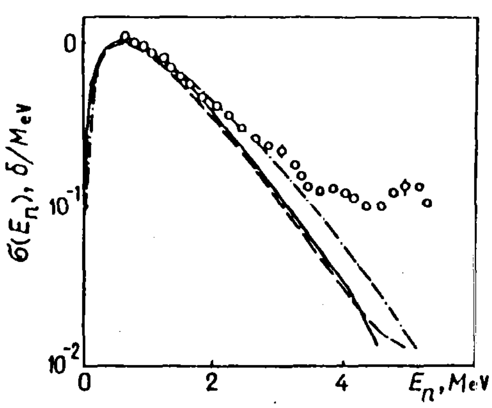

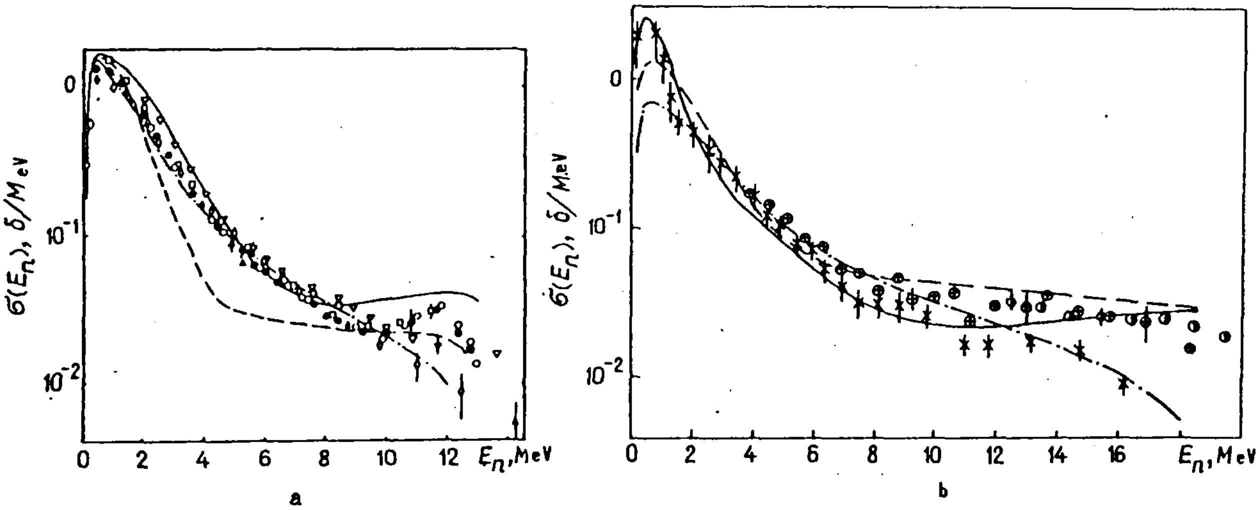

Fig. 5: Integral spectra of emission neutrons with an initial energy of approximately 14 MeV(a) and 20 MeV(b).
Experimental data: : Δ - [32]; □ - [33]; ● - [34]; ○ - [35]; ◊ - [36]; ∇ - [38]; x - [39]; ⊕ - [40]; ◑ - [41]. Evaluated data : —— - ENDL; ---- - ENDF/B-IV; -·-- INDL/V

be seen from Figs. 4 and 5, the evaluated data provide a satisfactory description of the experimental data in the region of scattered neutron energies below 2-3 MeV (it should be pointed out that the best description of the low-energy part of the neutron spectra is achieved by the INDL/V). In the high-energy part of the spectrum, appreciable inconformities are observed. As is shown by the theoretical analysis contained in Refs. [15, 42], this part of the spectrum is formed as a result of neutrons which have undergone direct inelastic scattering. Corresponding calculations, carried out according to the strong channel coupling model and in the distorted wave Born approximation, provide a satisfactory description both of the energetic and angular distributions of scattered neutrons. As is clear from Figs. 4 and 5, the pre-equilibrium decay model relationships contained in evaluated data file calculations provide a highly approximate description. In this respect a situation is typical when the incident neutron energy is 14 MeV. A result of the improved energy resolution achieved in recent work [33-35] has been that at this energy level too there has begun to appear, in the high energy part of the spectra, a structure which is highly uncharacteristic for a pre-equilibrium decay model. All this indicates that in the course of compiling evaluated data files it is necessary to use physically better-founded concepts of the interaction mechanism between neutrons and nuclei.

Analysis of the experimental data on the cross-sections for (n,n'), (n,2n) and (n,3n) reactions on ^{93}Nb, including research done in recent years, show that as a rule these data are in mutual agreement within the limits of experimental error. In cases where there are considerable divergences between the data of different authors, it is possible to point to uncertainties in the experimental method which produce systematic errors, and thus to discard these data.

Taking evaluated data on niobium from INDL/V, ENDF/B-IV, (ENDF/B-V) and ENDL and comparing it with experimental results leads to the following conclusions:

- Total and partial (with excitation of discrete groups of energy levels) neutron inelastic scattering cross-sections are represented with satisfactory accuracy in the INDL/V files;
- The cross-section for the (n,2n) reaction needs to be re-evaluated, taking account of the latest experimental data; the data in Ref. [29] can be recommended as a new evaluation. The evaluated emission neutron spectra unsatisfactorily reproduce the experimental data in the high-energy part of the spectra, in regard both to absolute size and to form (in the low-energy part the INDL/V evaluation can be recommended).

REFERENCES

[1] WRENDA 81/82: INDC (SEC)-78/URSF. Vienna, IAEA (1981).

[2] HERMSDORF, D. et al., Kernenergie, (1977), Bd 20, S. 166.

[3] PRONYAEV, V. et al., Report IAEA-NDS-31. Vienna, IAEA (1982).

[4] HOVERTON, R. et al., Report ANL/NDM-6. Argonne (1974).

[5] HOVERTON, R. et al., Report UCRL-50400. Livermore, 15 (1978).

[6] ABRAMOV, A.I., At. Ehnerg. 12 (1962) 62.

[7] GLAZKOV, N.P., ibid. 14 (1963) 400.

[8] BRODER, D.L. et al., ibid. 16 (1964) 103.

[9] GOBEL, H. et al., Z. Physik, (1970) Bd 240, S.430.

[10] VAN HEERDEN, I.J. et al., ibid. (1973) Bd 260, S.9.

[11] THOMSON, D.B., Phys. Rev., 129 (1963) 1649.

[12] HOPKINS, I.C. et al., Nucl. Sci. and Engng, 36 (1969) 275.

[13] COLES, R.E. Report AWRE-066/71. Aldermaston, (1971).

[14] BIRYUKOV, N.S. et al., Yad. Fiz. 19 (1974) 1201.

[15] SIMAKOV, S.P. et al., ibid. 37 (1983) 801.

[16] LYCHAGIN, A.A. et al., Preprint 1385, Institute of Physics and Energetics, Obninsk (1983) [In Russian].

[17] KOZYR', Yu.E. et al., Yad. Fiz. 26 (1977) 927.

[18] ROGERS, V.C. et al., Nucl. Phys., A142 (1970) 100.

[19] REITMANN, D. et al., ibid., 48 (1963) 593.

[20] ETEMAD, M.A. Report AE-481. Studvik, (1973).

[21] SMITH, A.B. et al., Z. Physik, (1973), Bd 264, S.379.

[22] PAULSEN, A. et al., ibid., (1970), Bd 238, S.23.

[23] HARING, M. et al., ibid., (1971), Bd 244, S.351.

[24] MATHER, D.S. et al., Report EANDC(UK)142 -AL. Vienna (1972).

[25] VESSER, L.R. et al., Phys. Rev., C16 (1977) 1792.

[26] FREHAUT, I. et al., Proc. symp. neutron cross-section from 10 to 50 MeV. Upton, 1 (1980) 399.

[27] HERMSDORF, D. et al., J. Nucl. Energy, 27 (1973) 747.

[28] HOLUB, E. et al., J. Phys., G2 (1976) 405.

[29] BYCHKOV, V.M. et al., Threshold reaction cross-sections caused by neutrons, Ehnergoizdat, Moscow (1982) [In Russian].

[30] STROHMAIER, B. Ann. Nucl. Energy, 9 (1982) 397.

[31] IWASAKI, S. et al., Proc. conf. nucl. cross-section for technology. Knoxville (1979) 73.

[32] VONACH, H. In: [26] 343.

[33] DEGTYAREV, A.P. et al., Yad. Fiz. 34 (1981) 209.

[34] TAKAHASHI, A. Report A-83-01. Osaka (1983).

[35] LYCHAGIN, A.A. et al., At. Ehnerg. 57 (1984) 266.

[36] SAL'NIKOV, O.A. et al., Vopr. At. Nauki i Tekh., Ser. Yad. Konstanty 7 (1971) 134.

[37] KAMMERDIENER, I.L. Report UCRL-51232. Livermore (1972).

[38] HERMSDO, D. et al., Report ZFK-277. Dresden (1974).

[39] PROKOPETS, G.A., in Neutron Physics: Material from the Fifth All-Union Conference on Neutron Physics, Kiev, 15-19 September 1980, TsNIIatominform 2 (1980) 54 [In Russian],

[40] LOVCHIKOVA, G.N. et al., Preprint 1603, Institute of Physics and Energetics, Obninsk (1984) [In Russian].

[41] MARCINKOWSKI, A. et al., Nucl. Sci. and Engng, 83 (1983) 13.

[42] LUK'YANOV, A.A. et al., Yad. Fiz. 21 (1975) 67.

Article submitted 28 September 1984.

TRANSMISSION FUNCTION MEASUREMENTS, EVALUATION OF MEAN RESONANCE PARAMETERS AND GROUP CONSTANTS FOR ^{235}U IN THE UNRESOLVED RESONANCE REGION

A.A. Van'kov, L.s. Gosteva, V.f. Ukraintsev, S. Toshkov, N. Yaneva

ABSTRACT

An analysis of experimental average transmission and cross-sections data for ^{235}U was carried out using the multilevel theory. A new evaluation for mean resonance parameters and group constants of ^{235}U was made in the energy region 0.1-21.5 keV.

Research is currently being done on analysing neutron cross-sections in the resonance energy region [1]. For fissile nuclides, the problem of the resonance region is complicated by the need to take account of the strong effects of inter-level interference. Uranium-235 is an example of one of these "difficult" nuclides. At the same time, the evaluation of its fission cross-section is taken as standard. The latest evaluation of the cross-sections for ^{235}U in the ENDF/B-V library [2] is connected with work [3] on the analysis of ^{235}U cross-sections for polarized neutrons. These results significantly affect the recommended values for mean resonance parameters: the mean distance between the levels D and the fission widths in the states J^{π}, equal to 3^-, 4^-.

The aim of the present work is to make a combined analysis of the data for ^{235}U using the mean cross-sections from Ref. [2] and of the results obtained by the authors of the present work for transmission function measurements of the type:

$$T(n) = 1/\Delta u \int exp\left[-\sigma_t(u)n\right]du\,; \qquad T_f(n) = 1/\langle\sigma_f\rangle \int \sigma_f(u) exp\left[\sigma_t(u)n\right]du\,,$$

and also to obtain an improved evaluation of the mean resonance parameters for ^{235}U. This will be used as the basis for calculating group constants (mean cross-sections and resonance self-shielding factors) for a system such as the BNAB-78 library [4].

Description of experimental data on transmission functions

The transmission T(n) and the self-indication functions of the fission reaction $T_f(n)$ were measured using the IBR-30 reactor neutron time-of-flight spectrometer. The neutron spectrum was close to the Fermi slowing-down spectrum. A description of the experimental conditions is given in Refs [5 and 6]. It should be noted that the sample filters, of metallic uranium, were 90% enriched and had high chemical purity.

We intend to analyse Garber's results [2] and the experimental data on the functions T(n) and $T_f(n)$ shown in Fig. 1, which also shows the data from Ref. [7]. Apart from ours, the latter is the only work in which the function $T_f(n)$ is measured for ^{235}U but it is measured only at neutron energies below 1 keV. There is good agreement between the results of Czirr's work [7] and our present data.

An evaluation of the errors in our results is given in Refs [5 and 6]. The main component of these errors is related to the background measurement. In analysing the experiment and in evaluating the mean resonance parameters, the errors for the experimental values T(n) and $T_f(n)$ emerged somewhat

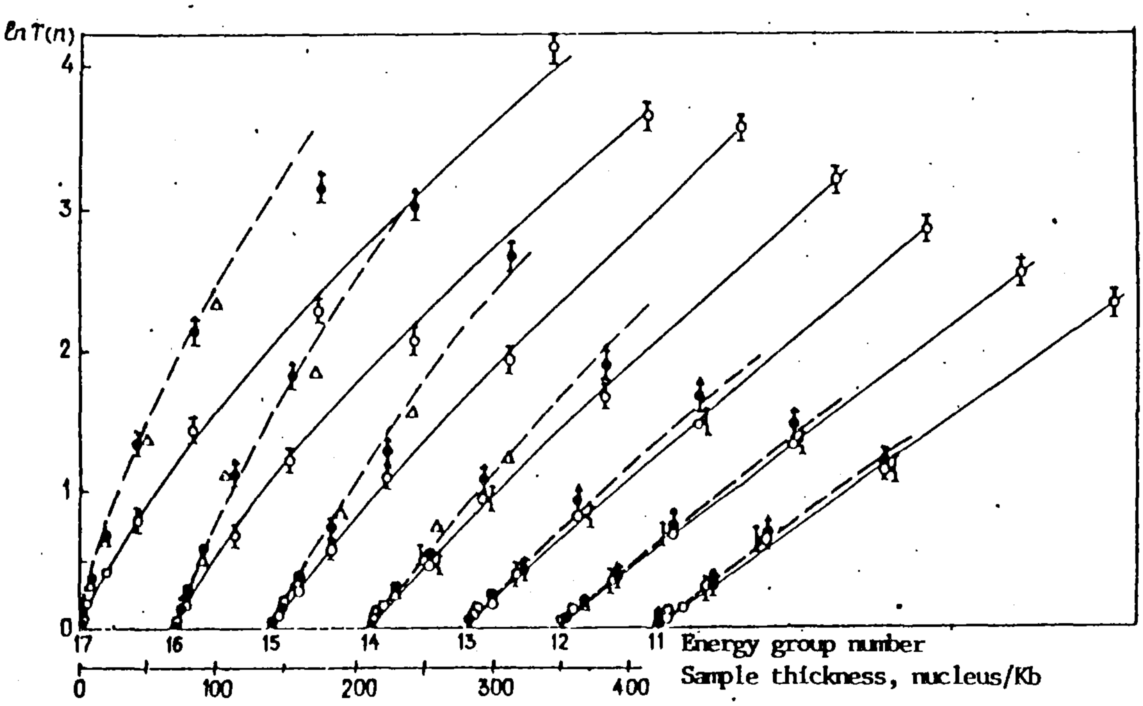

Fig. 1. Transmission functions (experimental points and optimized calculation)
Data of the present work: ɸ - $T(n)$; ϕ - $T_f(n)$. Data of Ref: [7]: Δ - $T_f(n)$

higher than those stated in Ref. [5]. These errors correspond to a confidence level of 95%.

Calculation-theoretical method. Calculation of the mean cross-sections based on the evaluated mean resonance parameters is usually performed using the Hauser-Feshbach formalism [8]. Bhat et al [9] obtain the mean resonance parameters for ^{235}U used in the files of the ENDF/B-V library and representating the initial data for calculating the recommended mean cross-sections. The present authors aimed to refine these parameters on the basis of additional experimental data on transmission functions. These values are sensitive to the effects of inter-resonance interference, and therefore the calculational model must take fairly strict account of them. Obviously the transmission functions cannot theoretically be calculated using the Hauser-Feshbach formalism. Moreover, only a multilevel formalism is suitable for this purpose. It was decided that the Reich-Moore formalism was here appropriate. It expresses the link between the neutron cross-sections and the S-matrix in the well-known way:

$$\sigma_t(E) = 2\pi \lambda^2 \sum_{J\pi} g(J) \sum_{\ell_j} (1 - Re\, S^{J\pi}_{n\ell_j, n\ell_j}) ;$$

$$\sigma_f(E) = \pi \lambda^2 \sum_{J\pi} g(J) \sum_{\ell_j} \left| S^{J\pi}_{n\ell_j, f\ell_j} \right|^2 ;$$

$$\sigma_{el}(E) = \pi \lambda^2 \sum_{J\pi} g(J) \sum_{\ell_j} \left| 1 - S^{J\pi}_{n\ell_j, n\ell_j} \right|^2 .$$

There is a unique relationship between the collision matrix S and the R-matrix which in the Reich-Moore approximation and has the form.

$$R_{cc'}(E) = \sum_{\lambda} \frac{\gamma_{\lambda c}\, \gamma_{\lambda c'}}{E_\lambda - E - i\bar{\Gamma}_\gamma/2},$$

where $\gamma_{\lambda c}$ is the amplitude of the reduced widths in the channel with the set of quantum numbers c; E_λ is the resonance energy; $\bar{\Gamma}_\gamma$ is the mean resonance width. The radiative capture cross-section was defined as the difference between the total cross-section and the fission and scattering cross-sections. This may account for the insignificance of interference effects in the radiative capture. In order to calculate the mean cross-sections and transmission functions using the Reich-Moore formalism, a method of statistical generation (Monte-Carlo method) of neutron cross-sections was developed. The authors describe the method in detail in Ref. [10].

Optimization method. The evaluation of the mean resonance parameters for ^{236}U was based on a combined analysis of the cross-sections in Ref. [2] and the transmission functions averaged in energy groups using the format of the BNAB-78 system of constants [4]. It is used in draft reactor calculations, and therefore the results obtained by the authors of the present work have practical significance. Moreover, the energy intervals (group widths) in this system are fairly large, which results in an averaging of the neutron cross-section fluctuations due to the resonance statistics and thereby ensures the correctness of the theoretical description in terms of the mean resonance parameters. The mean group cross-sections for ^{235}U from ENDF/B-V library file were obtained using the RECENT program. Optimization was performed using Bayes' method [11] which requires the following initial values:

- The initial a priori evaluation of the mean resonance parameters and their a priori error. The ENDF/B-V library evaluation [2] was taken for the values $\bar{D}$, S_o and Γ_γ, and the results in Ref. [12] for the other parameters. The errors were assumed to be 25% (for the parameter R' the error was assumed to be 5%);
- The deviation of the evaluated experimental data for the mean cross-sections and transmission functions from the calculated values;
- The errors in the evaluated experimental values for the mean cross-sections (5% for σ_f and 7% for σ_γ) and the transmission functions (2-3% for thin samples, increasing with the thickness of the sample to 20-30%). All the errors were reduced to the 95% confidence interval;

- sensitivity coefficients, i.e. the values $\frac{\partial \bar{F}_i}{\partial p_k} \Big/ \frac{\bar{F}_i}{p_k}$ where $\bar{F}_i$

  is the mean cross-section of transmission and P_k is the variable parameter of the model.

The following values varied: the mean distance [for various states the law of proportionality was assumed $\tilde{D}_J \sim (1/2J+1)^{-1}$], the mean radiation width $\bar{\Gamma}_\gamma$ (common to all states), the neutron strength functions S_o (varied in each group) and S_1 (independent of energy), and the fissile width Γ_f and $\ell = 0$ (varied in each group). The ratio of fission channel contributions also varied for the states with $\ell = 0$. The values Γ_f for $\ell = 1$ were fixed.

Description of the results The optimization results are given in Tables 1 and 2, and the fitting is shown in Table 3 and Fig. 1. Measurement of transmission functions for large thicknesses provides information about the scattering radius R', which in our model is assumed to be the same in all states. The optimization result showed the monotonic dependence of R' on neutron energies (see Table 2).

As is shown in Fig. 1 and Table 3, the parameters obtained provide a good description of the experimental material on mean cross-sections and transmission functions for ^{235}U. Figure 2 (continuous histogram) shows the calculation results for resonance self-shielding factors at room temperature based on optimized mean resonance parameters. The tabular data from the BNAB-78 libfary [7] are also shown there for comparison (broken line). It can be seen that the results of the authors' evaluation show a more pronounced resonance self-shielding effect for all ^{235}U reaction cross-sections.

Reliability of the evaluations. As a result of optimization, a covariation matrix of the D(p) parameters was obtained, which is not given here. Its diagonal elements characterize the a posteriori evaluation error. For the basic parameters such as S_o, $\bar{\Gamma}_\gamma$ and $\bar{\Gamma}_f$ ($\ell = 0$), the a posteriori errors never exceed 10% and the error of R' is less than 1.5%. The

Table I

Evaluation of non-energy dependent mean resonance parameters for ^{235}U (optimization result)

$J\pi$	D, eV	Γ_γ, MeV	$S_n \cdot 10^4$	Γ_f, eV	f_1	f_2
3^-	0,967	30	Var.	Var.	0,5	0,5
4^-	0,801	30	Var.	Var.	0,5	0,5
2^+	1,256	30	1,68	0,468	0,5	0,5
3^+	0,967	30	1,68	0,165	1,0	0,0
4^+	0,801	30	1,68	0,322	0,5	0,5
5^+	0,770	30	1,68	0,130	1,0	0,0

Note: f_1, f_2 - the ratio of fission channel contributions in the given state; Var. means that the parameter is variable in each energy group.

Table 2

Evaluation of the mean resonance parameters which are dependent on the number of the energy group (optimization result).

Number of group	Energy interval, keV	R', fm	$S_0 \cdot 10^{-4}$	$\bar{\Gamma}_f^{3-}$ MeV
11	10,0-21,5	9,1	1,05	153
12	4,65-10,0	9,2	0,964	170
13	2,15-4,65	9,2	0,901	243
14	1,00-2,15	9,2	0,910	170
15	0,465-1,00	9,2	1,05	176
16	0,215-0,465	9,2	0,940	144
17	0,100-0,215	9,5	0,950	120

Note: It is assumed that $\bar{\Gamma}_f^{3-} = \bar{\Gamma}_f^{4-}$.

Table 3

Mean cross-sections for ^{235}U in energy groups, b

Cross-section	Number of group						
	11	12	13	14	15	16	17
σ_t	15,0	16,6	18,5	22,3	28,3	35,9	44,5
	14,7	16,4	18,9	22,5	28,7	36,0	46,5
σ_γ	1,00	1,42	1,69	3,00	4,69	7,19	11,5
	1,08	1,38	1,69	2,94	4,61	7,33	11,5
σ_f	2,48	3,49	4,93	7,15	11,3	16,3	20,5
	2,56	3,45	5,18	7,15	11,5	16,0	21,5

Note: The numerator indicates the calculation from data in the ENDF/B-V library, the denominator indicates the optimized calculation.

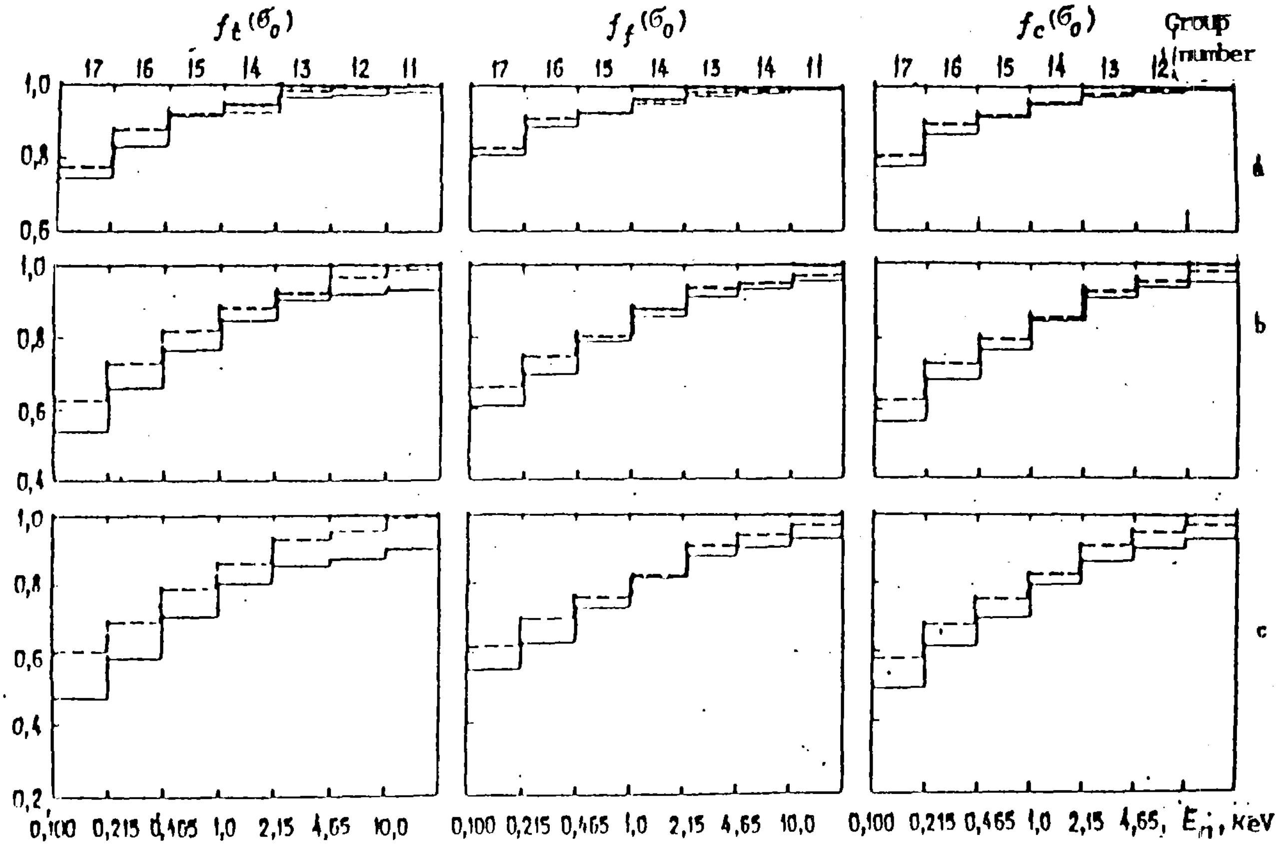

Fig. 2. Resonance self-shielding factors of total cross-section and of fission and capture cross-sections for ^{235}U at room temperature for dilution cross-sections σ_0, equal 100 b (a), 10 b (b) and 0 (c)

Table 4

Comparison of the discrepancies between the experimental (e) and optimized calculated (c) values of mean cross-sections with their a posteriori errors.

Energy Interval keV	$\bar{\sigma}_t$	$\bar{\sigma}_f$	$\bar{\sigma}_\gamma$
10-21,5	2,3	-3,1	-7,4
	1,9	5,7	5,7
4,65-10	1,4	1,2	2,9
	1,9	5,6	6,0
2,15-4,65	-2,3	-4,8	0,0
	1,9	5,2	5,8
1,00-2,15	-0,9	0,0	2,0
	2,0	5,1	5,7
0,465-1,00	-1,5	-2,2	1,7
	2,0	4,7	5,6
0,215-0,465	-0,3	2,3	-1,9
	2,0	4,1	5,6
0,100-0,215	-4,5	-4,9	0,4
	2,1	4,5	5,1

Note: The numerator indicates the discrepancy [(e-c)], %; the denominator indicates the a posteriori error, %.

Table 5

Comparison of the discrepancies between the experimental (e) and optimized calculated (c) transmission functions with their a posteriori errors.

Energy interval keV	0,02145	0,0858	0,1716
10-21,5	-0,6	-4,4	-2,1
	0,6	2,2	4,0
4,65-10,0	0,3	-2,3	-1,3
	0,6	2,3	4,1
2,15-4,65	1,5	-4,1	-1,8
	0,7	2,6	4,6
1,00-2,15	0,5	-6,2	-2,6
	0,8	2,6	4,4
0,465-1,00	0,0	-6,6	3,4
	1,0	2,8	4,5
0,215-0,465	1,0	-9,5	-4,0
	1,2	2,9	4,5
0,100-0,215	1,7	-5,2	17,7
	1,1	2,9	48

Note: The numerator indicates the discrepancy [(e-c)/c], %; the denominator indicates the a posteriori error, %.

reliability of the evaluation can be judged by comparing the a posteriori errors with the discrepancy between the results of the optimized calculation and the experimental evaluations (Tables 4 and 5). The a posteriori errors of F are obtained from the diagonal elements of the covariation matrix

$$D(p) : D(F) = K^{T} D(p) K,$$

where

$$K_{ij} = \frac{\partial F_i}{\partial p_j} \Big/ \frac{F_i}{p_j} \ .$$

The sensitivity coefficients were calculated using the perturbation method (in Monte Carlo calculations). Tables 4 and 5 show that the a posteriori errors obtained are comparable with the discrepancies in the experimental and optimized cross-sections and transmission functions. As the thickness of the sample increases, the tranmission measurement error significantly increases, and hence at specific points the discrepancy (e - c)/p may be 2-3 times greater than the a posteriori error. This is in agreement with the evaluations of the measurement errors, which exceed 10% for large thicknesses. On the whole, the data in Tables 4 and 5 demonstrate the self-consistency of the statistical errors and the reliability of the established confidence limits for the final results.

A high degree of accuracy was obtained a posteriori for the evaluation of resonance self-shielding factors: when σ_0 = 10 b, the relative error f_f and f_γ in the 17th group is 1.2%, further, the monotonic error falls as the energy increases, reaching 0.2% in the 11th group. When σ_0 = 100 b, the corresponding errors are 2-3 times less and have a similar dependence on energy.

When judging the evaluation errors, one has to take into account the fluctuation error in the mean functionals, caused by the natural statistics and the final number of resonances in the group. This error was evaluated in calculations using the Monte-Carlo method. At low energies (groups 16-17), it exceeds 10% for mean cross-sections, and for resonance self-shielding factors (where σ_o is 10 and 100 b) it is 4-8%. At higher energies, the fluctuation error becomes comparable to or less than the a posteriori error. The fluctuation error obviously does not play a role in the averaging of functionals over a wide spectrum. However, in the individual groups, it should be remembered that this error exists, and if it is to be removed, individual fitting must be made in each group permitting local (not physical) fluctuations of the mean resonance parameters.

On the basis of this analysis, the following conclusions can be drawn:

1. In comparison with the evaluations of the ENDF/B-V library, we obtained lower values for the radiation width $\bar{\Gamma}_\gamma$ (30 MeV instead of 35 MeV). For the p strength function, a single evaluation was obtained $S_1 = 1.667 \times 10^{-4}$. In the ENDF/B-V library the values quoted are $S_1 = 1.45 \times 10^{-4}$ ($J^\pi = 2^+, 5^+$) and $S_1 = 1.25 \times 10^{-4}$ ($J^\pi = 3^+, 4^+$). For a satisfactory description of the experimental material, the values S_o and Γ_f have to be varied separately in each group;

2. The best description is obtained by selecting the following fission channel contributions to the total fission width in the states 3^-, 4^-: $f_2 = 0.5$; $f_2 = 0.5$. We do not have any information on fission cross-sections in states with total momentum 3^-, 4^- and so the condition $\bar{\Gamma}_f^{3-} = \bar{\Gamma}_f^{4-}$ was adopted. Since there is only a slight difference in the momenta, this assumption seems reasonable. The selection of fission channel contributions and of the values of Γ_f for $\ell = 1$ has little effect on the optimization results;

3. From the experimental data on transmission functions, it follows that the scattering radius R' is monotonically dependent on neutron energy. If this effect is extracted from data only using $< \sigma_t >$, it is quite small;

4. The new evaluation obtained for mean resonance parameters for ^{235}U offers a good description of all the experimental data on mean cross-sections and transmission functions. Its reliability is characterized by the a posteriori covariation matrix from which the errors in the calculated group constants are obtained. It is recommended that practical use be made of the results when compiling more precise group constants.

REFERENCES

[1] VAN'KOV, A.A., Voprosi atomnoj nauki i tekhniki, Ser. Yadernye konstanty, 4, 53 (1983) 3-8.

[2] GARBER, D., ENDF-102; BNL-NCS-50496 Upton (1979).

[3] HEYWORTH, G.A., MOORE, M.S., In: Proc. of the intern. conf. Harwell (1979) 241-255.

[4] ABAGYAN, L.P., BAZAZYANTS, N.O., NIKOLAEV, M.N. et al, Gruppovye konstanty dlya rascheta reaktorov i zashchity. M.: Ehnergoizdat (1981).

[5] VAN'KOV, A.A., GRIGOR'EV, Yu.V., UKRAINTSEV, V.F., et al, Voprosy atomnoj nauki i tekhniki, Ser. Yadernye konstanty 4 35 (1979) 48-52.

[6] BAKALOV, T., ILCHEV, G., TOSHKOV, S. et al. Transmission and self-indication measurements with ^{235}U and ^{239}Pu in the 2 eV-20 keV energy region. NBS special publ. N.594, Washington (1980) 692-694.

[7] CZIRR, G.B., Nucl. Sci. and Engng 70 3 (1979) 307-308.

[8] HAUSER, W., FESHBACH, H., Phys. Rev. 87 (1952) 366-370.

[9] BHAT, M.R., Evaluation of ^{235}U neutron cross-sections and gamma-ray production data for ENDF/B-V: BNL-NCS-51184 (1980).

[10] VAN'KOV, A.A., TOSHKOV, S., UKRAINTSEV, V.F., et al. Voprosy atomnoj nauki i tekhniki. Ser. Yadernye konstanty 4 53 (1983) 18-25.

[11] VAN'KOV, A.A., Yadernye konstanty (1974) M: Atomizdat 16 (1974) 11-19.

[12] AMTSIPOV, G.V., KON'SHIN, V.A., SUKHOVITSKIJ, E.Sh., In: Nejtronnaya fizika (Proceedings of III All-Union Conference on Neutron Physics, Kiev 9-13 June 1975). M: TsNIIatominform (1976) 15-20.

Article submitted 27 August 1984.

AN EVALUATION OF THE SPONTANEOUS FISSION PROMPT NEUTRON SPECTRUM OF ^{252}Cf

G.S. Bojkov, V.I. Yurevich

ABSTRACT

An evaluation of the spontaneous fission prompt neutron spectrum of ^{252}Cf from 1 keV to 20 MeV is described. Variance-covariance matrices for a number of recent experimental data sets were constructed and used to evaluate the neutron spectrum following a Bayesian procedure. The evaluated spectrum is compared with various experimental and theoretical representations.

The spontaneous fission prompt neutron spectrum of ^{252}Cf is recommended as an international standard [1] and at present is widely used for solving practical and scientific problems. Periodically, it becomes necessary to conduct new evaluations of the shape of the spectrum. Among the recommendations regarding the prompt neutron spectrum of ^{252}Cf fission, the most widespread evaluation is that in Ref. [2], carried out in 1975 and included in the IRDF-82 international file of recommended nuclear data [3]. However, this evaluation no longer satisfies the demands made on nuclear physical standards, since the data on which it was based are considerably out of date; it lacks a covariance matrix of the evaluated spectrum, and no account is taken of the results of integral measurements. These same faults are also inherent in the more recent Soviet evaluation [4]. At the international meeting held in 1983 [5], the need was identified for carrying out a new evaluation of the ^{252}Cf neutron spectrum.

The purpose of the present work is to evaluate the shape of the ^{252}Cf spontaneous fission prompt neutron spectrum, using the most recent experimental information on the basis of a detailed analysis of partial errors. The evaluation method applied is founded on a Bayesian approach [6], which makes it possible to calculate the covariance matrix of the evaluated spectrum from information on the correlations of experimental errors.

Evaluation method

The energy spectrum of the fission neutrons $\varphi(E)$ is presented in a form convenient for conducting the evaluation

$$\varphi(E) = \mu(E)\,\varphi_M(E), \tag{1}$$

where $\varphi_M(E) = 0.667\ E^{1/2} \exp(-E/T)$, with T = 1.42 MeV for the ^{252}Cf fission neutron spectrum, and E is the neutron energy in MeV. The function $\varphi_M(E)$, called a scale function, satisfactorily describes the shape of the neutron spectrum in the region of the basic spectral integral 0.5-6 MeV [2]. Thus, the spectral form structure function $\mu(E)$ is the one which has to be evaluated.

When carrying out an evaluation of continuous functions, for example the energy dependence of any reaction cross-section, it is customary to seek a particular set of discrete values of the function, assigned to the corresponding energy network of small dimensions, which considerably facilitates the evaluation procedure by avoiding work with large matrices. The values of the function at intermediate energies can be found by the prescribed interpolation rules. A similar procedure can conveniently be used when evaluating the form of the fission neutron spectrum, the function $\mu(E)$.

In the present work we have used a method of evaluation based on a general procedure for refining nuclear data [6-8]. For each independent vector of input experimental data $\vec{D}$, the correspondening covariance matrix V is formed on the basis of their partial errors. In the case of a non-linear function $\vec{D}(\vec{X})$, where $\vec{X}$ is the set of experimental parameters,

$$V = \langle (\delta\vec{D})(\delta\vec{D})^{+} \rangle = S \langle (\delta\vec{X})(\delta\vec{X})^{+} \rangle S^{+}, \tag{2}$$

where S is a sensitivity matrix with elements $S_{ij} = (X_j/D_i)\ (\partial D_i/dX_j)$.

Finding the "best" evaluation of the parameter vector $\vec{P}'$ and its covariance matrix M' is based on Bayes' theorem. The problem amounts to deriving a vector $\vec{P}'$ such as to minimize the expression

$$q^2 = (\vec{P} - \vec{P}')^+ M^{-1}(\vec{P} - \vec{P}') + (\vec{D} - \vec{D}')^+ V^{-1}(\vec{D} - \vec{D}'), \tag{3}$$

where $\vec{D}' = \tilde{\vec{D}} + G(\vec{P}' - \vec{P})$. The vector $\tilde{\vec{D}}$ can be found by the parameter vector $\vec{P}$, using the functional link $\vec{D} = \vec{D}(\vec{P})$, and the elements of the sensitivity matrix G have the form $G_{ij} = \partial D_i/\partial P_j$. The method of deriving a refined parameter vector $\vec{P}'$ and the corresponding covariance matrix M on the basis of expression (3) is called the generalized least-squares method and amounts to solving the following equations

$$\begin{aligned} (\vec{P}' - \vec{P}) &= MG^+ [N + V]^{-1}(\vec{D} - \tilde{\vec{D}}); \\ M - M' &= MG^+ [N + V]^{-1} GM , \end{aligned} \tag{4}$$

where $N = GMG^+$. When evaluating the shape of the fission neutron spectrum, the evaluated parameter vector $\vec{P}$ will be represented by the vector $\vec{\mu}$, the elements of which are the values of the shape function $\mu(E)$ on the energy network selected. When refining the spectrum by adding the results of differential spectrometry, the vector $\vec{\mu}_e$ will be the data vector $\vec{D}$. Normalization of the relative energy distribution of neutrons per unit area can be carried out by the equations

$$\begin{aligned} \vec{\mu}_{norm} &= \vec{\mu} + MG^+ N^{-1}(1 - J); \\ M_{norm} &= M - MG^+ N^{-1} GM , \end{aligned} \tag{5}$$

where $J = \int_0^{20\ \mathrm{MeV}} \varphi(E)dE = \sum_i J_i$, and the elements of the sensitivity matrix G have the form $G_i = \partial J/\partial \mu_i = J_i/\mu_i$. When adding the integral data, the vector $\vec{D}$ will be represented by the set of experimental average cross-sections for n reactions:

$$\vec{\bar{\sigma}}_e = \begin{pmatrix} \bar{\sigma}_{e1} \\ \vdots \\ \bar{\sigma}_{en} \end{pmatrix} \tag{6}$$

The values $\bar{\sigma}$, $\sigma(E)$ and $\varphi(E)$ are connected by the relationship

$$\bar{\sigma} = \int_0^{20\,\mathrm{MeV}} \sigma(E)\varphi(E)dE = \int_0^{20\,\mathrm{MeV}} \sigma(E)\mu(E)\varphi_M(E)dE \tag{7}$$

where the normalization condition $\int_0^{20\,\mathrm{MeV}} \mu(E)\varphi_M(E)dE = 1$ is fulfilled, and therefore when adding new data on $\vec{\bar{\sigma}}_e$ not only the spectrum will be refined but also the reaction microscopic cross-sections. In this case the evaluated parameter vector $\vec{P}$ will consists of two sub-vectors $\vec{\sigma}$ and $\vec{\mu}$:

$$\vec{P} = \begin{bmatrix} \vec{\sigma} \\ \vec{\mu} \end{bmatrix}, \tag{8}$$

where the vector $\vec{\sigma}$ itself consists of n sub-vectors (n reactions). If initially vectors $\vec{\sigma}$ and $\vec{\mu}$ are independent, then the covariance matrix M can be represented in block form as

$$M = \begin{bmatrix} M^{\sigma} & 0 \\ 0 & M^{\mu} \end{bmatrix}, \tag{9}$$

and the sensitivity matrix G as

$$G = \left[G^{\sigma}\, G^{\mu} \right], \tag{10}$$

the elements of which are $G^{\sigma}_{ij} = \partial\bar{\sigma}_i/\partial\sigma_j$; $G^{\mu}_{ij} = \partial\bar{\sigma}_i/\partial\mu_j$. If one is interested only in refining the shape of the spectrum, it can be shown that the new values $\vec{\mu}'$ and $M^{\mu'}$ are found by solving equations similar to equations (4):

$$\begin{aligned} (\vec{\mu}' - \vec{\mu}) &= M^{\mu}G^{\mu+}\left[N+V\right]^{-1}(\vec{\bar{\sigma}}_e - \vec{\bar{\sigma}}_c); \\ M^{\mu} - M^{\mu'} &= M^{\mu}G^{\mu+}\left[N+V\right]^{-1}G^{\mu}M^{\mu}, \end{aligned} \tag{11}$$

where $N = G^{\sigma}M^{\sigma}G^{\sigma+} + G^{\mu}M^{\mu}G^{\mu+}$, and $\vec{\bar{\sigma}}_c$ is the vector of the calculated mean reaction cross-sections. If vectors $\vec{\sigma}$ and $\vec{\mu}$ are initially dependent, the covariance matrix has the form

$$M = \begin{bmatrix} M^{\sigma} & M^{\mu\sigma+} \\ M^{\mu\sigma} & M^{\mu} \end{bmatrix}. \tag{12}$$

The refined vector $\vec{\mu}'$ and the corresponding covariance matrix $M^{\mu'}$ are found from equations (11), only matrix N will have the form

$$N = G^{\sigma}M^{\sigma}G^{\sigma+} + G^{\mu}M^{\mu\sigma}G^{\sigma+} + (G^{\mu}M^{\mu\sigma}G^{\sigma+})^{+} + G^{\mu}M^{\mu}G^{\mu+}. \tag{13}$$

Analysis of experimental work

A detailed analysis of all experimental uncertainties is the essential basis for carrying out an updated evaluation of the ^{252}Cf neutron standard spectrum, calling for the construction of a reliable covariance matrix of errors [5]. The ever more strict requirement for an accurate knowledge of the shape of the spectrum has led experimenters to direct their main efforts to the careful conduct of measurements and to the minimization of and correct allowance for various types of uncertainty [9-14]. A critical examination of the experimental material has shown that in the majority of publications devoted to research on this spectrum comparatively little attention is paid to an analysis of errors in measurement results. This applies both to work carried out by the time-of-flight method (e.g. [15, 16]) and to studies performed by the amplitude method, and likewise to integral measurements [17]. For example, in the case of Ref. [18], the results of which were taken as basic for evaluation [2], we were unable to evaluate the magnitude of the basic errors.

The studies selected [9-14] are characterized by the following features, which conveniently distinguish them from other work:

- The high experimental level of the precision measurements, which are supported by the best and most recent methodological treatment and the latest nuclear-physical data;
- The availability of preliminary research and the wealth of information contained in the material published by the authors;
- Considerable efforts to solve problems of optimizing the set-up of measurements, and minimization of and correct allowance for various types of uncertainty;
- A lengthy critical analysis of the results obtained;
- Good agreement of the results;
- A set of measurements covering the energy range from 1 keV to 20 MeV.

In spite of the above-listed merits of these studies it has nevertheless been necessary to expend a considerable effort on collecting from various sources the information required for conducting the evaluation, and also on a re-analysis of the experimental errors, with a view to identifying the correlations present.

Time-of-flight measurement method. A short description of Refs [9-13] is given in Table 1. In these studies measurements were carried out under substantially different experimental conditions, each with its own particular type of neutron detector. Hence, these results can be regarded as mutually independent. A list of the uncertainties considered for each study is given in Table 2. Some of the uncertainties listed were broken down into more elementary items when the file of errors was constituted. Errors in the efficiency of the neutron detector for all the studies is one of the basic errors, an analysis of which in respect of studies [11-13] constituted a highly complex task. In evaluating the correlation coefficients for the efficiency values at various neutron energies three levels were used: 0; 0.5; 1.

In Refs [9, 10], the shapes of the neutron spectra were determined relative to the standard cross-sections for the $^{6}Li(n,\alpha)$ and $^{235}U(n,f)$ reactions; for this purpose use was made of data from the ENDF/B-V file [19]. The results of these measurements were considered in those regions for which cross-sections are recommended for the reactions in question. In performing the analysis of errors use was also made of the results of studies [20-22].

In Ref. [11] the spectrum in the energy region above 4 MeV was measured only in one series using a large black neutron detector, and below 4 MeV three series of measurements were carried out, two of them using a small black neutron detector. The authors of the present study assumed that the efficiencies in these energy regions are poorly intercorrelated. To analyse

Table 1   Short description of studies used for evaluation

Study	Time resolution ns/m	Flight length, m	Source strength, fiss./s	Detector system	Energy range, MeV	Energy range used in evaluation, MeV	Observations
[9]	3 6 12 24	0.5 0.25 0.125 0.0625	~1x10^5 ~2x10^4	Fragment detector: a low-mass gas scintillation counter with good separation of alpha particles from fragments. Neutron detector: composed of ^{6}Li I(Eu) crystals, 17.5 mm diameter and 2 and 4 mm thick. Efficiency: ^{6}Li(nα) reaction cross-section. ENDF/B-V file used.	0.001-2	0.001-0.2 0.3-0.4	Relative measurements. Use made of energy region where the ^{6}Li (n,α) reaction cross-section is standard. In the 0.2-0.3 MeV resonance peak region and above 0.5 MeV the cross-section has considerable uncertainty.
[10]	1.7 3.4	1 0.5	2.0x10^5 5.1x10^5	Fragment detector: ionization chamber of mass less than 1 g. Neutron detector: low-mass (~ 65 g) ionization chamber with ^{235}U layers. Efficiency: ^{235}U (n,f) reaction cross-section. ENDF/B-V file used.	0.01-14	0.1-10	Relative measurements. Use made of energy region where the ^{235}U(n,f) reaction cross-section is standard. Above 10 MeV the data show considerable uncertainty in comparison with the results of Refs [12, 13].
[11]*	~1.3	2.6 3.5	1.4x10^5	Fragment detector: large scintillation camera. Neutron detector: small and large black detectors. Efficiency: calculated.	0.2-10	0.5-6	Relative measurements. Use made of energy region where the corrections are small in comparison with the spectral intensity.
[12]*	0.125	12	~1x10^5	Fragment detector: ionization chamber, mass ~1 g. Neutron detector: four detectors based on an NE-213 liquid organic scintillator, dimensions Ø 25.4 x 5.08 cm with light guide. Experimental efficiency used (threshold ~ 1.6 MeV).	3-13	4-13	Absolute measurements. Data in the 3 MeV region not used in evaluation owing to their considerable divergence beyond the limits of error) from the results given in the Tables to Refs [10,11,15,18].

* Numerical data taken by the authors from the figures, which in these papers are of high quality.

Table 1 (continued)

Study	Time resolution ns/m	Flight length, m	Source strength, fiss./s	Detector system	Energy range, MeV	Energy range used in evaluation, MeV	Observations
[13]	~0.44	4.5	$3.3x10^4$	Fragment detector: small-mass ionization chamber. Neutron detector: NE-213 liquid organic scintillator, diameter 12 x 12 cm. Efficiency: calculated. Measurements conducted in five series with various sets of lower (~7-10 MeV) and upper (~17-22 MeV) thresholds.	11-30	11-20	Relative measurements. In the energy region above 20 MeV the results are not very convincing (30 events to 15 background events) and contain considerable errors.

Table 2

Uncertainties in studies [9-13]

Type of uncertainty	[9]	[10]	[11]	[12]	[13]
Statistical error	X	X	X	X	X
Differential non-linearity	+	+	+	+	+
Uncertainty of time channel value	+	+	+	+	+
Uncertainty of "time zero"	+	X	X	X	X
Uncertainty of flight length	+	+	+	+	+
Uncertainty of neutron detector efficiency	X	X	X	X	X
Uncertainty of correction for genuinely random coincidences	+	+	X	+	+
Uncertainty of correction for neutron scattering in the air medium	X	+	+	+	+
Uncertainty of correction for neutron scattering by the detectors	X	+	+	+	+
Uncertainty of correction for neutron scattering by removed masses	+	+	X	+	+
Uncertainty of correction for final time resolution	+	X	X	+	+
Uncertainty of normalization of different series of measurements	X	-	-	-	-
Uncertainty introduced by the (n/γ) separation channel	-	-	X	+	+
Uncertainty associated with incomplete recording of fission events	+	+	X	+	+
Uncertainty of correction for background reactions and delayed gamma quanta	X	-	-	-	-
Uncertainty of correction for anisotropy of emergence of ^{235}U fission fragments and kinematic effect	-	+	-	-	-

Note: The sign "X" means that the uncertainty makes a substantial contribution to the total error; the signs "+" and "-" represent respectively the presence or absence of the uncertainty in question.

the errors in the calculated detector efficiencies, recourse was had to the results of the experimental testing of the calculated efficiency of a small black detector [23], and also to the results of a comparison, conducted by the present authors, of the experimental data in Refs [24, 25] on the $^{235}U(n,f)$ reaction cross-section with the evaluated values for this cross-section contained in Refs [8, 19, 26, 27]. In the energy region around 3-4 MeV, an additional efficiency error (of about 3%) was introduced, equal in size to the discrepancy between the experimental and the evaluated figures for the

$^{235}U(n,f)$ reaction cross-section. For analysis of the errors use was further made of the results of studies [28-30].

The absolute measurements in Ref. [12] were carried out with four identical neutron detectors. The experimental absolute efficiency of the detectors was used, the value of which somewhat exceeds that of the calculated efficiency [31]. The present authors evaluated the following partial errors: statistical systematic error of the absolute efficiency, and also the uncertainty in the shape of the efficiency curve. At the same time some information was derived from comparing the experimental and calculated neutron detector efficiencies (with reference to the NE-213 scintillator and with a neutron detection threshold around 1.5 MeV) [12, 32-34]. In analysing the experimental uncertainties recourse was also had to the results of studies [35-40].

In relative measurements [13] the neutron detector efficiency was calculated by a code described in Ref. [14], which is analogous to the widely used code figuring in Ref. [42]. The counter efficiency uncertainty was evaluated on the basis of studies [43-47]; for establishment of correlations, it was assumed that the basic contribution to this uncertainty is made by two types of partial error, associated with uncertainty regarding the detection threshold and the uncertainty of the data on the breakdown of carbon nuclei entering into the composition of the detector organic scintillator. For analysis of the experimental uncertainties recourse was had to the results of Refs [43-48]. The results of the works considered above were not corrected. We only eliminated what were from our point of view unlikely results located at the boundaries of the measurement energy range (see Table 1).

Integral measurements. For an extensive set of dosimetric reactions having a threshold energy lower than 10 MeV, Ref. [14] provides a joint evaluation of the mean cross-sections measured in the ^{252}Cf neutron field. For the evaluated figures a covariance matrix of errors was constructed, and the results are presented in a form convenient for inclusion in the evaluation. Study [14] also includes highly accurate measurements of the mean cross-sections for (n,2n) reactions with a threshold energy above 10 MeV. The missing components of the correlation matrix for a set of mean reaction cross-sections, including the results of measurements in Ref. [14] for (n,2n) reactions, were determined by us using the data from Refs [7, 49, 50]. For assigning the values of the reaction microscopic cross-sections and the covariance error matrices corresponding to them, use was made of data from the ENDF/B-V and IRDF-82 files. The microscopic cross-sections for the various reactions were considered to be independent, in view of the fact that there was no information on correlations between them (except the ^{197}Au(n,2n) and ^{59}Co(n,2n) reactions, for which the cross-sections were formed essentially from the results of Ref. [51], and the correlation coefficient was assumed to be 0.5). It should be noted that for many reactions the evaluated cross-section files do not contain covariance error matrices, or else the values for the errors substantially exceed the uncertainty of measurement by time-of-flight [9-13] or the cross-sections for other reactions sensitive to the same energy range. Hence, for inclusion in the evaluation a limited set of reactions was chosen (Table 3). As may be imagined, the values for the mean cross-sections $\bar{\sigma}_e$ and microscopic cross-sections $\sigma(E)$ for the selected reactions are much more reliable and consistent with respect to the results of Refs [9-13], carried out by the time-of-flight method. In the energy range corresponding to the greatest uncertainty of the differential spectrometry data, the results of the integral measurements given in Table 3 make it possible to refine the neutron spectral shape under evaluation.

Analysis of evaluation

As starting information in the present evaluation, use was made of the relative data from four studies [9-11, 13] and the absolute data in study [12], obtained by the time-of-flight method, and also the set [14] of mean cross-sections for nine reactions (see Table 3). The results of the

Table 3

Short description of reactions used in the evaluation

Reaction	Energy region corresponding to the 90% integral of the reaction response function in the ^{252}Cf spectrum, MeV	$\bar{\sigma}_e$, mb	$\delta\bar{\sigma}_e$, %	$\delta\bar{\sigma}_c$, %	$\sigma(E)$ - source
$^{197}Au(n,\gamma)$	0.066-3.0	76.17	2.0	8.7	ENDF/B-V
$^{27}Al(n,p)$	3.5-9.8	4.825	3.2	5.6	ENDF/B-V
$^{56}Fe(n,p)$	5.5-12	1.446	2.1	4.5	ENDF/B-V
$^{27}Al(n,\alpha)$	6.5-12	1.004	1.9	2.9	[54]
$^{197}Au(n,2n)$	8.9-14.8	5.461	2.2	~5	[51]
$^{59}Co(n,2n)$	~11-16	0.406	2.5	~5	[51-55]
$^{63}Cu(n,2n)$	~12-17	0.183	3.8	1.7	IRDF-82
$^{19}F(n,2n)$	~12-17	1.63×10^{-2}	3.1	2.6	IRDF-82
$^{90}Zr(n,2n)$	~13-18	0.221	2.7	2.0	IRDF-82

studies carried out by the time-of-flight method were entered onto Fig. 1 in the form of the relationship $\mu(E) = \varphi(E)/\varphi_M(E)$, where $\varphi_M(E)$ is the scale function (1). The agreement of results was checked visually. The studies considered, and also earlier investigations carried out with high time resolution [15, 18, 52, 53] show an absence of fine structure, going beyond the limits of experimental error, in the case of the prompt neutron spectrum for ^{252}Cf spontaneous fission. On these grounds we assume that the function of the spectral shape for evaluation represents a fairly smooth energy function. The experimental data in Fig. 1 show that all the features of the spectral shape can be well described by assigning the values of the function $\mu(E)$ at the nodes of a small energy network, taking account of the linear interpolation rule for obtaining values at the intermediate energies. The authors chose an energy network consisting of 20 nodes, covering the energy range 0-20 MeV (Table 4). The results of Refs [9-13] were applied to this energy network by transferring them parallel to the smooth curve drawn through the set of experimental points.

In the first stage of the evaluation, a covariance matrix of total errors taking account of expression (2) was formed for each study. In the

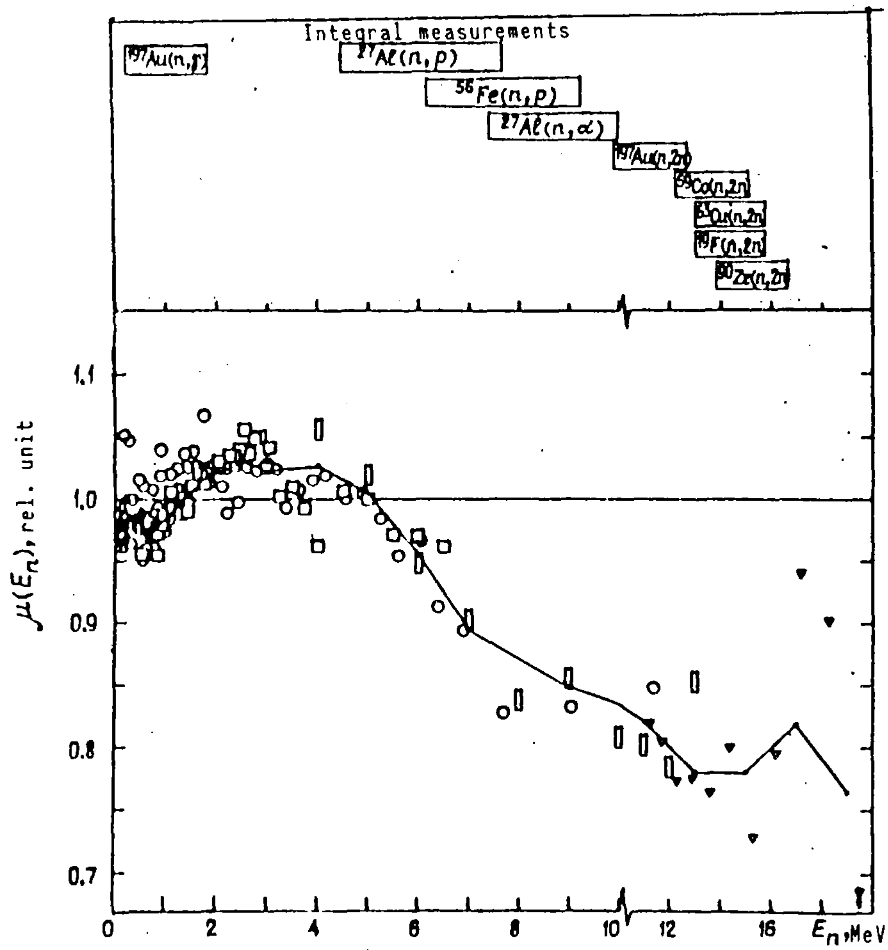

Fig. 1. Comparison of the evaluated curve for the shape function μ(E) (continuous curve) with the input data from time-of-flight spectrometry: Δ - [9] [measured relative to the $^6Li(n,\alpha)$ reaction cross-section]; O - [10] [measured relative to the $^{235}U(n,f)$ reaction cross-section; □ - [11]; Ⅱ - [12]; ∇ - [13]. The upper part of the figure represents schematically the energy intervals corresponding to these data, and also shows the energy regions corresponding to the 60% integral of the response function for the nine dosimetric reactions used in the evaluation.

next stage we derived the values $\mu_i = \mu(E_i)$, i = 1, 2, ..., 20 from the results of relative measurements [9-11, 13]. The integral of the neutron energy distribution derived φ(E) was normalized to unity. Then, to the normalized data were added the results of the absolute measurements [12]. All the procedures for addition and normalization of data were effected under the conditions of the generalized least squares methods on the basis of expressions (4), (5).

Further refinement of the spectral shape function μ(E) was carried out by adding the results of the integral measurements quoted in Table 3.

Table 4

Evaluated figures and correlation matrix for the ^{252}Cf spectral shape function

i	E_i, MeV	$\mu_i \pm \Delta\mu_i$	Correlation matrix																			
1	0.004	0.9628±0.0550	100																			
2	0.02	0.9952±0.0480	75	100																		
3	0.06	0.9771±0.0418	60	70	100																	
4	0.15	0.9820±0.0353	35	40	50	100																
5	0.30	0.9872±0.0276	45	45	55	45	100															
6	0.70	0.9712±0.0153	-5	-5	-10	-5	-5	100														
7	1.20	0.9944±0.0094	-30	-30	-35	-30	-35	-5	100													
8	1.80	1.0177±0.0102	-25	-25	-30	-30	-40	-10	70	100												
9	2.50	1.0305±0.0137	-20	-20	-25	-25	-30	-40	-15	-20	100											
10	3.00	1.0234±0.0155	-20	-20	-25	-30	-35	-35	-20	-15	70	100										
11	4.00	1.0270±0.0178	-10	-10	-15	-20	-30	-20	-25	-20	5	10	100									
12	5.00	1.0039±0.0183	-5	-10	-10	-10	-20	-20	-20	-15	0	0	35	100								
13	6.00	0.9553±0.0196	-5	-5	-5	-10	-15	-15	-25	-15	-10	0	30	50	100							
14	7.00	0.8937±0.0186	-5	-5	-5	-10	-15	-10	-15	-5	0	-10	20	40	45	100						
15	9.00	0.8477±0.0200	-5	-5	-5	-10	-15	0	-20	-10	-5	-5	25	35	45	50	100					
16	11.00	0.8198±0.0260	-5	-5	-5	-10	-15	-10	-10	0	0	0	15	20	35	45	55	100				
17	13.00	0.7799±0.0308	0	0	-5	-5	-10	-5	0	-5	-5	5	5	15	20	25	30	35	100			
18	15.00	0.7800±0.0562	0	0	0	0	0	0	0	0	0	0	0	0	0	5	5	0	-15	100		
19	17.00	0.8190±0.1060	0	0	0	0	0	0	0	0	0	0	5	0	5	0	5	5	-10	-20	100	
20	19.00	0.7650±0.3570	0	0	0	0	0	0	0	0	0	0	0	0	0	0	-5	-5	-15	-45	-20	100

Table 5

Representation of shape function $\mu(E)$

ΔE, MeV	$\mu(E)$
0-0.3	0.975+0.04 E
0.3-0.7	0.987+0.04 (0.3-E)
0.7-1.0	0.971+0.043 (E-0.7)
1.0-2.5	1.010+0.017 (E-1.0)
2.5-4	1.030+0.003 (2.5-E)
4-5	1.025+0.021 (4-E)
5-7	1.004+0.055 (5-E)
7-13	0.894+0.019 (7-E)
13-20	0.700

Table 6

Relative error in the values for the function $\mu(E)$

ΔE, MeV	$\delta\mu$, %	ΔE, MeV	$\delta\mu$, %
0-0.01	5.7	3.5-4.5	1.7
0.01-0.04	4.8	4.5-5.5	1.8
0.04-0.10	4.3	5.5-6.5	2.1
0.10-0.225	3.6	6.5-8	2.1
0.225-0.50	2.8	8-10	2.4
0.50-1.0	1.6	10-12	3.2
1.0-1.5	0.95	12-14	4.0
1.5-2.1	1.0	14-16	7.2
2.1-2.7	1.3	16-18	13
2.7-3.5	1.5	18-20	47

Addition of the integral data was effected on the basis of expression (11). The ^{197}Au(n,γ) reaction was utilized for refining the spectrum in the low energy range, taking account of the delayed neutron contribution (Appendix 1).

Discussion of results

The numerical values for the evaluated quantities $\mu(E)$ on the selected energy network and the corresponding correlation matrix for the ^{252}Cf spontaneous fission prompt neutron spectrum are given in Table 4. The integral of the evaluated spectrum is normalized to unity. For practical applications it is more convenient to use a simpler representation of the results obtained, ignoring the small and statistically insignificant fluctuations in the spectral shape (Table 5). The errors in the values $\mu(E)$ for various energy ranges are given in Table 6, and the corresponding correlation matrix can be taken from Table 4.

One of the most important parameters characterizing the energy distribution of neutrons is the mean energy. The mean energy $\bar{E}$ and the square of its error var($\bar{E}$) can be derived using the expression:

$$\bar{E} = \int_0^{20\,MeV} E\varphi(E)dE = \int_0^{20\,MeV} E\mu(E)\varphi_\mu(E)dE = \sum_{i=1}^{20} I_i \mu_i ;$$

$$var(\bar{E}) = \sum_i (I_i)^2 var(\mu_i) + 2\sum_{\substack{i \\ (i<j)}}\sum_j I_i I_j cov(\mu_i \mu_j) .$$

Using the data in Table 4, a mean energy and error value $\bar{E}$ = 2.1214 ± 0.0122 MeV was derived for the evaluated spectrum of ^{252}Cf spontaneous fission prompt neutrons. The degree of agreement of the evaluated shape of the spectrum with the results of time of flight spectrometry can be visually estimated from Fig. 1. Figure 2 shows the results of testing the evaluated spectrum for its agreement with the data for a comprehensive set of dosimetric reactions. The experimental values of the mean cross-sections ($\bar{\sigma}_e \pm \Delta\bar{\sigma}_e$), measured in the ^{252}Cf spectrum, were taken from Ref. [14], and the data for the microscopic cross-sections were taken from the ENDF/B-V file. The quantity D/U was determined by the expression:

$$D/U = \frac{\bar{\sigma}_e - \bar{\sigma}_c}{\left[(\Delta\bar{\sigma}_e)^2 + (\Delta\bar{\sigma}_c^{\sigma})^2 + (\Delta\bar{\sigma}_c^{\varphi})^2\right]^{1/2}} , \qquad (15)$$

where $\bar{\sigma}_e$ and $\bar{\sigma}_c$ are the experimental and calculated values for the

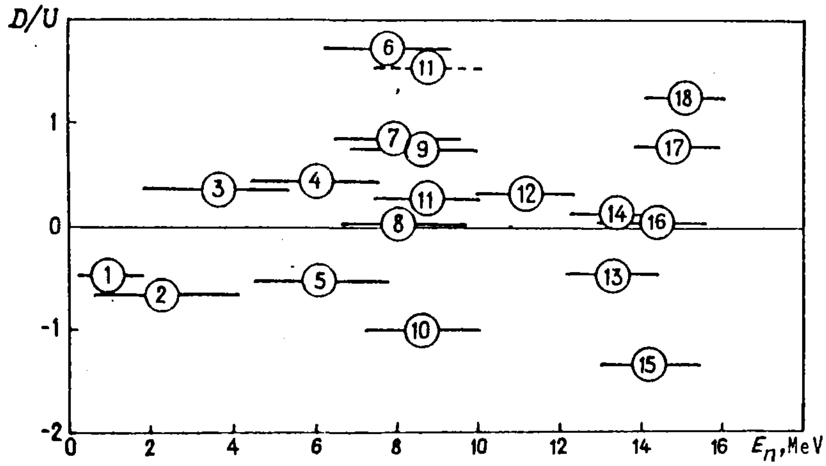

Fig. 2. Comparison of the calculated values for the mean cross-sections $\overline{\sigma}_c$ with the experimental values $\overline{\sigma}_e$ using expression (15) for a large set of dosimetric reactions: 1 - ^{197}Au(n,γ); 2 - ^{235}U(n,f); 3 - ^{238}U(n,f); 4 - ^{46}Ti(n,p); 5 - ^{27}Al(n,p); 6 - ^{56}Fe(n,p); 7 - ^{48}Ti(n,p); 8 - ^{63}Cu(n,α); 9 - ^{59}Co(n,α); 10 - ^{24}Mg(n,p); 11 - ^{27}Al(n,α) (the dotted line denotes the value of D/U, for deriving which use was made of the cross-section σ(E) from Ref. [54]; 12 - ^{197}Au(n,2n); 13 - ^{55}Mn(n,2n); 14 - ^{59}Co(n,2n); 15 - ^{63}Cu(n,2n); 16 - ^{19}F(n,2n); 17 - ^{90}Zr(n,2n); 18 - ^{58}Ni(n,2n). The energy intervals represented correspond to the 60% integral of the reaction response function in the ^{252}Cf neutron spectrum.

mean cross-section; $\Delta\overline{\sigma}_c^{\varphi}$ and $\Delta\overline{\sigma}_c^{\sigma}$ are the uncertainties in the calculated mean cross-section associated with the uncertainty in the spectral shape φ and the microscopic cross-section σ respectively; and $\Delta\sigma_e$ is the error in the experimental value of the mean cross-section. As can be seen from the figure, for most reactions this value lies within the range [-1,+1], which indicates the good agreement of the evaluated shape of the spectrum with the values used for the mean and microscopic reaction cross-sections. It should be noted that for the ^{197}Au(n,γ) and ^{235}U(n,f) reactions the contribution of delayed neutrons was taken into account when calculating the mean cross-section.

Figure 3 compares the results of the present work with the evaluations in Ref. [2] and the latest recommendation [5], in which, below 6 MeV, it is proposed to use a function of form μ = 1, and above 6 MeV a function of the form taken from evaluation [2] (the dashed lines delimit the area of possible

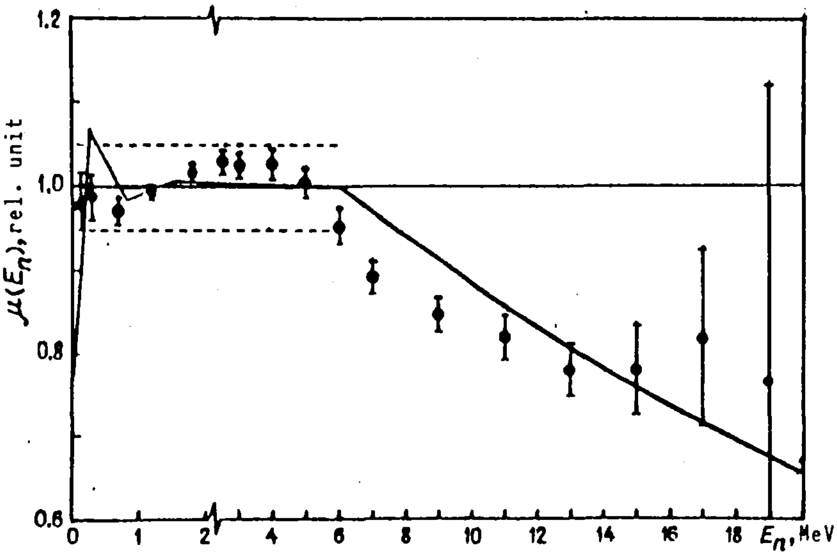

Fig. 3. Comparison of the evaluated function of the ^{252}Cf prompt neutron spectral shape (•) with the results of the evaluation in Ref. [2] (thin curve) and the recommended values [5] (bold curve, coinciding above 6 MeV with the results of study [2]).

Table 7

Relative contribution of delayed neutrons to intensity of spectrum

ΔE, keV	<1	1-105	105-225	225-500	500-950	950-1500	>1500
N_{del}/N_{pr}, %	<0.1	0.161	0.646	0.955	0.716	0.166	<0.1

Table 8

Initial error matrix for the $^{197}AU(n,\gamma)$ reaction cross-section

ΔE, MeV	$\delta\sigma$, %	Correlation matrix				
0.05-0.5	6.1	1				
0.5-0.6	4.1	0.04	1			
0.6-1.0	4.1	0.04	0.06	1		
1.0-2.5	20.0	0	0	0.19	1	
2.5-3.5	20.0	0	0	0	0.96	1

Table 9

Error matrix obtained after refining the $^{197}Au(n,\gamma)$ reaction cross-section

ΔE, MeV	$\delta\sigma$, %	Correlation matrix					
0.05-0.225	6.03	1					
0.225-0.5	6.03	0.01	1				
0.5-1.0	4.0	-0.05	0.01	1			
1.0-2.15	7.3	-0.56	-0.40	-0.10	1		
2.15-2.75	8.0	-0.50	-0.36	-0.08	0.73	1	
2.75-3.5	8.7	-0.45	-0.32	-0.52	0.77	1	1

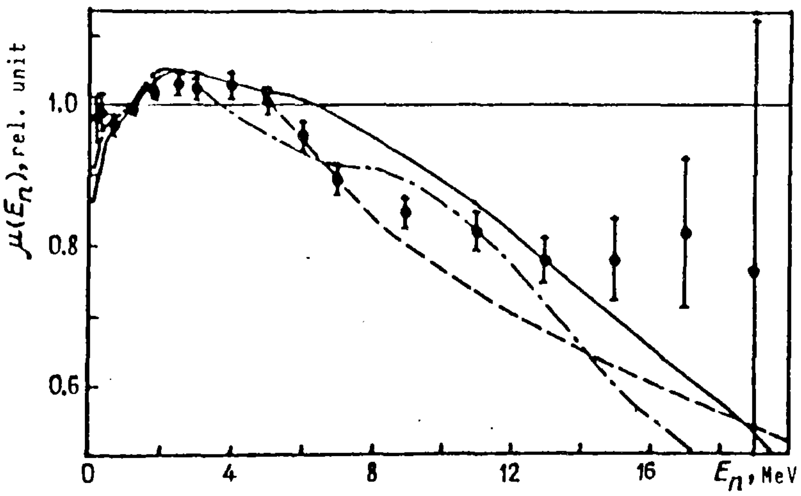

Fig. 4. Comparison of the evaluated function of ^{252}Cf prompt neutron spectral shape (•) with the results of model calculations ——— – [58] (version 3); – – – – [57]; and –·–·– – [59].

variations in the spectral shape). In the energy range below 6 MeV, the shape of the evaluated spectrum agrees, within the limits of the uncertainties indicated, with the recommendations contained in Ref. [5] and largely derived on the basis of those same experimental data. The functions μ(E) evaluated in the present work and in Ref. [2], and describing the low-energy part of the spectrum, have different aspects; the divergence in their values reaches 8% for an energy of 0.250 MeV and 20% for an energy below 100 keV. In the energy range 1.5-5 MeV, the values obtained by us for the spectral shape function systematically exceed the evaluation values [2], to an extent of about 4%, and in the energy range 6-12 MeV our evaluated values for the μ(E) function lie systematically lower (the divergence amounts to about 7%) than the representation in Ref. [2]. For neutron energies above 12 MeV, Ref. [2] postulates a hypothetical shape for the spectrum derived from extrapolation into the higher energy region of the analytical representation of the function μ(E), determined from experimental data in the 6-12 MeV range. In this energy range the spectral intensity evaluated in the present study agrees within the limits of error with the values derived from the relation μ(E) postulated in Ref. [2].

Thus, our evaluated function for the shape of the ^{252}Cf spontaneous fission prompt neutron spectrum, while agreeing with the experimental data and the results of the recommendation contained in Ref. [5], has a somewhat different aspect in comparison with the representation contained in Ref. [2], and a substantially reduced uncertainty in the energy regions below 0.250 MeV and above 8 MeV. The covariance matrix derived for the evaluated values (see Table 4) shows that the uncertainty in the form of the energy distribution of ^{252}Cf prompt neutrons in the energy range 0.225-11 MeV does not exceed 3%, and in the 0.01-14 MeV range it is less than 5%. The accuracy achieved meets the demands made on neutron standards, and makes it possible to use the spectrum for calibration purposes in various items of nuclear physics research. Appendix 1 deals with the matter of deriving the absolute intensity of the spectrum and allowance for the contribution of delayed neutrons.

Recently, together with experimental investigation of fission neutron spectra, great effort has been applied to deriving theoretical representations of spectra with the help of various model calculations [56-59]. It will be seen from Fig. 4 that the neutron energy distributions obtained are in good agreement over a wide energy range with our evaluations in the present paper. However, it should be pointed out that all the above-mentioned theoretical calculations were carried out on the basis of the evaporational model and contain model parameters, a reasonable variation of which leads to a substantial change in the calculated neutron energy distribution (the discrepancy amounts to tens of per cent in the energy region above 5 MeV) [57, 58]. Hence the theoretical calculations to some extent require fitting. For example, in study [58] fitting was carried out to the experimental data of study [15] by selection of an energy level density parameter a and subsequent correction of the calculated spectrum was effected using the results of the integral measurements in Ref. [60]. In addition, the theoretical spectral separation representations in question were derived without taking account of the contribution of the so-called separation

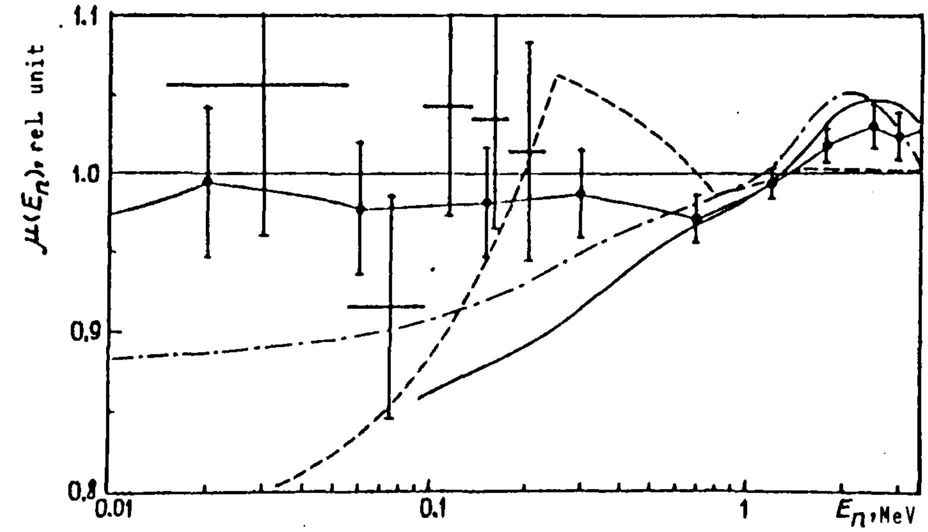

Fig. 5. Low-energy region of the ^{252}Cf spontaneous fission prompt neutron spectrum. The evaluated function of the shape $\mu(E)$(Φ) is compared with the results of absolute measurements [16] (—┼—) (only data for the energy region below 200 keV are shown), and averaging is carried out over the intervals shown on the figure with the evaluation from Ref. [2] (– – – –) and the calculations in Ref. [58] (———) and [59] (–•–•–).

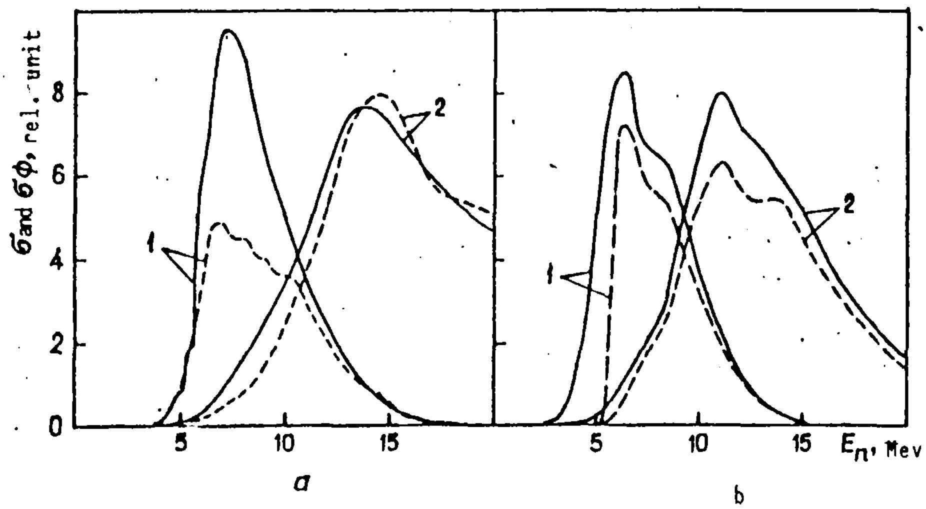

Fig. 6. Cross-sections and corresponding response functions in the neutron fission spectrum for the $^{48}Ti(n,p)$ (a) and $^{63}Cu(n,\alpha)$ (b) reactions: 1 - reaction response functions $\sigma(E)\Phi(E)$; 2 - reaction microscopic cross-sections $\sigma(E)$; – – – – data for $\sigma(E)$ from ENDF/B-IV file; ——— - data from ENDF/B-V file.

neutrons, the available information about which is scanty and frequently contradictory [57].

The low energy region of the ^{252}Cf neutron spectrum is examined in Fig. 5. Within the limits of error, the experimental data agree with the evaluated shape of the spectrum. However, as can be seen from the figure, the results obtained in the present work regularly lie higher than those of Ref. [2] and the theoretical calculations, particularly in the energy range below 100 keV.

* *

*

The present work has been devoted to deriving an evaluated shape of the ^{252}Cf spontaneous fission prompt neutron energy distribution in the energy range 1 keV-20 MeV, on the basis of a detailed analysis of experimental errors. The evaluated data, on the one hand, are in good agreement with the experimental results, and on the other hand do not contradict theoretical representations, agreeing over a wide range of energies with the calculated values. On the whole, the spectral shape function derived does not contradict the recommendation recently drafted at an international meeting [5] and, so it appears, can be regarded as the next stage in refining the standard neutron spectrum in comparison with the evaluation contained in Ref.[2]. The numerical data, including the correlation matrix, quoted in the tables for the ^{252}Cf prompt neutron spectrum may be widely used in assignments associated with refinement of various nuclear physical constants. An example of such an assignment on refining dosimetric reaction cross-sections is given in Appendix 2.

Appendix 1

Derivation of absolute spectral intensity and allowance for the delayed neutron contribution

In order to determine the absolute intensity, pertaining to each fission event, of the ^{252}Cf neutron spectrum, it is necessary to use the expression $\Phi_{pr}(E) = \bar{\nu}_{pr}\varphi_{pr}(E)$. Here $\bar{\nu}_{pr} = 3.757 \pm 0.006$ neutr./fiss. and is the average number of prompt neutrons per ^{252}Cf fission event (value taken from ENDF/B-V file); $\varphi_{pr}(E) = \mu_{pr}(E)\varphi_{M}(E) = \mu_{pr}(E)\ 0.667\ \sqrt{E}\ \exp\ (-E/1.42)$, where $\mu_{pr}(E)$ is the evaluated function of the spectral shape, and E is the neutron energy in MeV.

The intensity of the total ^{252}Cf neutron spectrum can be established by adding the delayed neutron spectrum to the evaluated prompt neutron spectrum. In the present work, for determining the shape of the delayed neutron spectrum $\varphi_{del}(E)$, use was made of the data quoted in Ref. [61]. The intensity of the delayed neutron spectrum is found as $\Phi_{del}(E) = \bar{\nu}_{del}\varphi_{del}(E)$, where $\bar{\nu}_{del} = 0.89 \times 10^{-2}$ neutr./fiss. is the mean number of delayed neutrons per ^{252}Cf fission event (value taken from ENDF/B-V file). Then we have $\Phi_{tot}(E) = \Phi_{pr}(E) + \Phi_{del}(E)$.

Table 7 shows the ratio of the number of delayed neutrons to the number of ^{252}Cf fission prompt neutrons for several energy intervals. It will be seen that the intensity of the total neutron spectrum is only slightly different from that of the prompt neutron spectrum. This makes it possible to use the covariance matrix of the prompt neutron evaluated spectrum likewise for the total spectrum in various applications.

Application of the evaluated spectrum for refinement of dosimetric reaction cross-sections

Over a wide energy range, the errors derived by us in this paper for the evaluated values of the standard ^{252}Cf neutron spectrum are considerably smaller than the uncertainties in the cross-sections of the majority of dosimetric reactions. For many of these reactions the values for the mean cross-sections measured in the ^{252}Cf neutron spectrum are known with a high degree of accuracy (the error represents only a few per cent) [14], which makes it possible to refine their microscopic cross-sections $\sigma(E)$. In case of joint refinement of the cross-sections for n reactions, the vectors of the new data and evaluated parameters will be respectively

$$\vec{\bar{\sigma}}_e = \begin{pmatrix} \bar{\sigma}_{e1} \\ \vdots \\ \bar{\sigma}_{en} \end{pmatrix} \quad \text{and} \quad \vec{\sigma} = \begin{pmatrix} \vec{\sigma}_1 \\ \vdots \\ \vec{\sigma}_n \end{pmatrix},$$

where $\bar{\sigma}_{ei}$ is the experimental mean cross-section of the i-th reaction, and $\vec{\sigma}_i$ is the vector of the microscopic cross-section of the i-th reaction. The new parameter vector and covariance matrix corresponding to it are found using the expressions

$$\vec{\sigma}' = \vec{\sigma} + M^{\sigma} G^{\sigma +} \left[N + V\right]^{-1} (\vec{\bar{\sigma}}_e - \vec{\bar{\sigma}}_c) ;$$
$$M^{\sigma'} = M^{\sigma} - M^{\sigma} G^{\sigma +} \left[N + V\right]^{-1} G^{\sigma} M^{\sigma},$$

As an example of the above procedure in action, let us consider refinement of the ^{197}Au(n,γ) reaction cross-section. To the initial cross-section $\sigma(E)$ we add new information obtained in the integral measurements in the ^{252}Cf neutron spectrum: $\bar{\sigma}_e = 76.17 \pm 1.52$ mb [14]. The energy range where the reaction is most sensitive to the neutron spectrum is normally characterized by an energy interval corresponding to the 90% integral of the response function, which in the case of the ^{197}Au(n,γ) reaction is equal to 0.066-3.0 MeV for the ^{252}Cf neutron spectrum. It is clear that in this energy region refinement of the microscopic cross-section for the reaction in question will basically occur. The numerical data describing the form of the neutron spectrum are taken from Table 4, allowing for the delayed neutron contribution, and for determining the microscopic cross-section values and corresponding error matrix (Table 8) use was made of the ENDF/B-V file.

Since the calculated and experimental average cross-sections were close to one another in magnitude, the new values for the microscopic cross-section derived in the refinement process scarcely differ from the initial values (maximum divergence about 1%). However, the uncertainty of the cross-section after addition of the integral data is substantially reduced for neutron energies above 1 MeV. Table 9 shows the errors for the refined cross-section values and the new correlation matrix.

The majority of (n,p), (n,α) and (n,2n) dosimetric reactions have a threshold above a few MeV, where the intensity of the neutron fission spectrum rapidly falls with increasing energy. The product of the neutron spectrum $\Phi(E)$ and the cross-section for such a reaction $\sigma(E)$ and the function, increasing with energy, near the threshold leads to a relatively narrow response function $\sigma(E)\Phi(E)$, the maximum of which is assignable to the energy region near the threshold. Therefore the most effective refinement of the cross-section upon addition of the data from integral measurements will take place in the range a few MeV above the reaction threshold. As an example of the great sensitivity of the reaction response function to the values of its cross-section near the threshold, we give in Fig. 6 data corresponding to various representations of the microscopic cross-sections for the ^{48}Ti(n,p) and ^{63}Cu(n,α) reactions.

REFERENCES

[1] Prompt fission neutron spectra. Vienna: IAEA, 1972, p.169; WRENDA 81/82: INDC(SEC)-78/URSF, Vienna: IAEA, 1981.

[2] Grundl J.A., Eisenhauer C.M. In: Proc. Inter. conf. on nuclear cross-sections and technology (Washington, 1975). NBS special publ. 425, 1975, v.1. p.250; IAEA-TECDOC-208, 1978, v.1, p.53.

[3] Cullen D.E., Kocherov N.P., McLaughlin P.M. Nucl. Sci. and Engng, 1983, v.83, p.497.

[4] STAROSTOV, B.I., SEMENOV, A.F., NEFEDOV, V.N., Vopr. At. Nauki i Tekh., Ser. Yad. Konstanty 2 (1980) 3.

[5] IAEA consult meeting on the ^{235}U fast-neutron fission cross-section and the ^{252}Cf fission neutron spectrum (Smolenice, 1983): INDC(NDS)-146/L, 1983, p.23.

[6] Dragt J.B., Dekker J.W., Gruppelaar H., Janssen A.J. Nucl. Sci. and Engng, 1977, v.62, p.117.

[7] Mannhart W. Report PTB-FMRB-84, 1981.

[8] Bhat M.R. In: [5], p.119.

[9] BLINOV, M.V., BITENKO, V.A., YUREVICH, V.I., in Neutron Physics (material from the Fifth All-Union Conference on Neutron Physics, Kiev, 15-19 September 1980), M.: TSNIIatominform 3 (1980) 109; ZfK-410 (1980) 104.

[10] Blinov M.V., Boykov G.S., Vitenko V.A. In: Proc.Intern. conf. on nuclear data for science and technology (Atworp., 1982): ECSC, EEC, EAEC, Brussels and Luxembourg, 1983, p.479; in: [5], p.161.

[11] Poenitz W.P., Tamura T. In: [10], p.465; in: [5], p.175.

[12] Bottger R., Klein H., Chalupka A., Strohmaier B. In: [10], p.484.

[13] Marten H., Seeliger D., Stobinski B. In: [10], p.488; INDC(GDR)-17/L, 1982.

[14] Mannhart W. In: [10], p.429.

[15] Boldeman J.W., Culley D., Cawley R.J. Trans. Amer. Nucl. Soc., 1979, v.32, p.733.

[16] Lajtai A., Dyachenko P.P., Kutzneva L.S. e.a. In: [5], p.177.

[17] DESZO, Z., CSIKAI, J., in Neutron Physics (material from the Fourth All-Union Conference on Neutron Physics, Kiev, 18-22 April 1977), M.: TSNIIatominform 3 (1977) 32; INDC (NDS)-103/M (1979) 176.

[18] Green L., Mitchell J.A., Steen N.M. Nucl. Sci. and Engng, 1973, v.50, p.257.

[19] INDC/NEANDC Nuclear standards file, version'80: INDC-36/LN, 1981, p.A-5, A-18.

[20] BLINOV, M.V., BITENKO, V.A., DUSHIN, V.N., YUREVICH, V.I., Vopr. At. Nauki i Tekh., Ser. Yad. Konstanty 1 (1981) 81.

[21] BLINOV, M.V., VITENKO, V.A., YUREVICH, V.I., See [9] 4 (1980) 86.

[22] Blinov M.V., Vitenko V.A., Dushin V.N., Yurevich V.I. Nucl. Instrum. and Methods, 1982, v.198, p.455.

[23] Wasson O.A., Meier M.M., Duvall K.C. Ibid., 1982, v.81, p.196.

[24] Poenitz W. Ibid., 1974, v.53, p.370.

[25] Poenitz W. Ibid., 1977, v.60, p.894.

[26] Poenitz W. Report ANL/NDM-45, 1979.

[27] Dushin V.N., Fomichev A.V., Kovalenko S.S. e.a. In: [5], p.53.

[28] Poenitz W. Nucl. Instrum. and Methods, 1973, v.109, p.413.

[29] Poenitz W. Report ANL-7915, 1972.

[30] Lamaze G.P., Meier M.M., Wasson A.O. In: [2], p.73.

[31] Dietze G., Klein H. Report PTB-ND-22, 1982.

[32] Fowler J.L., Cookson J.A., Hussain M. e.a. Nucl. Instrum. and Methods, 1980, v.175, p.449.

[33] Haouat G., Lachkar J., Sigaud J. e.a. Ibid., 1978, v.65, p.331.

[34] Nakayama K., Pessoa E.F., Douglas R.A. Ibid., 1981, v.190, p.555.

[35] Chalupka A. Ibid., 1979, v.164, p.105.

[36] Klein H. In: ZfK-491. Dresden, 1982, p.113.

[37] Bottger R., Brede H.G., Cosack M. e.a. In: [10], p.532.

[38] Schlegel-Bickmann D., Dietze G., Scholermann H. Nucl. Instrum. and Methods, 1980, v.169, p.517.

[39] Chalupka A., Strohmaier B., Klein H., Bottger R. In: [5], p.187.

[40] Klein H., Bottger R., Chalupka A., Strohmaier B. In: [5], p.191.

[41] Hermsdorf D. In: ZfK-315. Dresden, 1977, p.192.

[42] Stanton N.R. Report COO-1545-92,1971.

[43] Marten H., Seeliger D., Stobinski B. In: [36], p.122.
[44] Abdel-Wahab M.S., Bialy J., Schmidt F.K. Nucl. Instrum. and Methods, 1982, v.200, p.291.
[45] Gul K. Ibid., 1980, v.176, p.549.
[46] Cecil R.A. e.a. Ibid., 1979, v.161,p.439.
[47] Del Guerra A. Ibid., 1976, v.135, p.337.
[48] Marten H., Seeliger D., Stobinski B. In: [5], p.195.
[49] Mannhart W. Nucl. Sci. and Engng, 1981, v.77, p.40.
[50] Kobayashi K., Kimura I., Mannhart W.J. Nucl. Sci. Technol., 1982, v.19, p.341.
[51] Frehaut J., Bertin A., Bois R., Jary J. In: Symposium on neutron cross-sections from 10 to 50 MeV: BNL-NCS-51245, 1980, v.1, p.399.
[52] Scobie J., Scott K.D., Feather N., Vass D.G. J. Phys. G: Nucl. Phys., 1977, v.3, p.1443.
[53] Guenther P., Havel D., Sjoblom R., Smith A. Report ANL/NDM-19, 1976.
[54] Tagesen S., Vonach H. In: [19], p.A-22.
[55] Veeser L.R., Arthur E.D., Young P.G. Phys. Rev. C, 1977, v.16, p.1791.
[56] Browne J.C., Dietrich F.S. Ibid., 1974, v.10, p.2545.
[57] Marton H., Neumann D., Seeliger D. In: [5], p.199.
[58] Madland D.G., Nix J.R. Nucl. Sci. and Engng, 1982, v.81, p.213; In: [10], p.473.
[59] Batenkov O.I., Blinov M.V., Boykov G.S. e.a. In: [5], p.161.
[60] LaBauve R.J., Madland D.G. Trans. Amer. Nucl. Soc., 1983, v.44, p.538.
[61] Sephier D., Ilberg D., Shalev S., Yiftah S. Nucl. Sci. and Engng, 1977, v.62, p.660.

Article submitted 26 June 1984

ANGULAR AND ENERGY DISTRIBUTIONS OF ^{252}Cf SPONTANEOUS FISSION NEUTRONS

E.A. Seregina, P.P. D'yachenko

ABSTRACT

Methods are described for measuring the energy distributions of ^{252}Cf spontaneous fission neutrons using a single-crystal recoil proton spectrometer, and for reconstructing neutron spectra from the instrumentally-derived distributions with the inclusion of a realistic spectrometer response function. The energy spectra obtained are shown for ten angles between the direction of motion of the neutrons and the axis of emergence of the fragments (3°, 10°, 20°, ..., 90°) within the energy range 0.7-8.1 MeV. Comparison of the results obtained with data from other authors showed that the picture of angular and energy distributions of ^{252}Cf spontaneous fission neutrons is somewhat different from that previously established. This applies particularly to angles between the fragment emergence axis and the direction of the neutrons which are close to 0° and 90°.

Experimental data on the angular and energy distributions of ^{252}Cf spontaneous fission neutrons are of great value in testing and developing existing models of the mechanisms for prompt fission neutron emission. However, these distributions are studied in sufficient detail in only one work [1] (carried out in 1962), in which neutron spectra are measured for 16 angles between the directions of emergence of the neutrons and the light fragment in the range $0^{\circ} < \theta < 180^{\circ}$ in steps of 11.25°. No experiments have been carried out in such detail since then, and evidence has been accumulating that the actual angular and energy distributions are somewhat different from those established in Ref. [1]. For example, according to the data in Ref. [2], in which the angular yield correlations and differential energy distributions of spontaneous ^{252}Cf fission neutrons were measured, the neutron spectra for angles of $\theta > 30^{o}$ have a mean energy significantly lower than that obtained in Ref. [1].

We therefore considered it worth while repeating the detailed study of the angular and energy distributions of prompt ^{252}Cf spontaneous fission neutrons using a method for measuring the spectrum different from those employed in Refs [1] and [2]; the method chosen involved the use of a single-crystal recoil proton spectrometer with a stilbene crystal. It should be noted that it is of major importance to use several methods in a study of such complexity, as this is, of course, the only way to detect whether any of the systematic errors which must necessarily occur in any method have not been taken into consideration.

Measurement method

The experiment consisted of two stages. In the first stage the spectra of the ^{252}Cf fission neutrons were measured simultaneously for six angles, 3^{o}, 10^{o}, 20^{o}, 30^{o}, 80^{o} and 90^{o}, between the direction of neutron emission and the axis of emergence of the fission fragments, and in the second stage for angles of 40^{o}, 50^{o}, 60^{o}, 70^{o}, 80^{o} and 90^{o}. To determine the directions of motion of the fragments, silicon surface barrier counters were used which were 0.2 mm thick and had working surface diameters of 14 mm and external diameters of 18 mm. The semiconductor counters were manufactured from n-type silicon of 300 Ohm-cm resistivity using the technology described in Ref. [3]. The surface barrier detectors were positioned within a thin- walled vacuum chamber made of Duralumin in a circle at a distance of 107 mm from a layer of fissile material. A layer of ^{252}Cf 4 mm in diameter with an emission rate of 3×10^{4} fissions/s was deposited on a platinum support 0.05 mm thick. For the neutron detector, a crystal of stilbene measuring 22 x 31 mm was used, together with a photomultiplier. For γ-quanta discrimination, (n-γ) separating circuit [4] was used, which suppressed the γ-quanta close to the threshold level by a factor of 50 and by more at higher energies. The threshold of the detector was 0.7 MeV.

It was known that the (n-γ) separation circuit was sensitive to changes in ambient temperature. This effect was excluded by placing the detector in a thermostat kept at a temperature of $26^{o} \pm 0.5^{o}$C, which significantly increased the stability of the neutron channel. The neutron detector was placed at a distance of 25 cm from the fissile material target. The geometry of the experiment enabled an angular resolution of $\pm(4\text{-}5^{o})$ to be achieved. The solid angle of neutron detection was then 0.0144 sr.

The measurements were carried out with the help of the Physics Measurement Centre (PMC) of the Physics and Energy Institute. Six independent spectrometer channels were linked to six fragment detectors with an additional channel to the neutron detector (Fig. 1). The amplitude signal from the neutron detector was fed to the analog-to-digital converter which was controlled by the signal from the detector number encoder. In this way, the six neutron spectra from the apparatus, corresponding to the six angles being measured, were fed into the PMS magnetic operating store.

Measurement procedure

The experiment was carried out in cycles. Each cycle consisted of two types of measurement: measurement of the background effect and measurement of the scattered neutron background using a copper shadow cone placed between the ^{252}Cf target and the neutron detector. The duration of each type of measurement was 23 hours. At the beginning and end of each 23-hour series, the following control measurements were made:

1. The amplitude distribution of the Compton recoil electrons formed as a result of the interactions of γ-quanta from ^{137}Cs (E = 480 eV) and ^{60}Co (E = 1.33 MeV) with the stilbene crystal was measured in order to calibrate the neutron spectrometer and to monitor the stability of the electronic apparatus. The stability

Neutron energy distributions $n(E_n,\theta_\lambda)$ as a function of emission angle in the laboratory system, neutr./fiss·sr·MeV.

E_n, MeV	3°	10°	20°	30°	40°	50°	60°	70°	80°	90°
0,7	25,00±I,86	22,56±I,67	26,80±I,68	22,53±I,4I	25,00±I,89	23,80±I,69	I6,77±0,97	I6,74±0,97	I6,18±I,29	I7,28±I,35
0,9	2I,4I±0,86	25,00±0,69	28,39±0,62	25,I0±0,56	24,30±0,58	22,02±0,5I	I6,68±0,50	I5,96±0,47	I3,94±0,35	I4,80±0,37
I,I	26,67±0,58	27,72±0,26	30,46±0,28	27,I0±0,25	23,44±0,35	I8,90±0,27	I6,06±0,40	I4,6I±0,35	I2,32±0,28	I2,65±0,29
I,3	3I,08±0,70	3I,3I±0,7I	3I,90±0,73	28,I2±0,64	22,60±0,59	I6,78±0,44	I4,94±0,44	I2,96±0,38	I0,98±0,28	I0,74±0,28
I,5	33,6I±0,86	33,30±0,85	32,06±0,82	27,82±0,72	2I,35±0,59	I5,40±0,43	I3,59±0,38	II,28±0,32	9,63±0,27	9,I0±0,26
I,7	35,06±I,08	33,80±I,04	3I,64±0,97	26,95±0,82	20,I0±0,64	I4,08±0,45	I2,29±0,38	9,83 ±0,30	8,44±0,27	7,72±0,25
I,9	35,44±I,I6	33,74±I,II	30,70±I,00	25,65±0,84	I8,78±0,62	I2,84±0,43	II,02±0,37	8,54±0,29	7,35±0,26	6,55±0,24
2,I	34,96±I,08	33,07±I,02	29,4I±0,9I	24,08±0,75	I7,40±0,54	II,65±0,36	9,80±0,34	7,38±0,26	6,36±0,23	5,58±0,20
2,3	33,94±0,98	32,06±0,92	27,97±0,8I	22,44±0,65	I6,07±0,49	I0,47±0,3I	8,68±0,3I	6,39±0,23	5,50±0,I9	4,75±0,I7
2,5	32,46±0,8I	30,7I±0,77	26,37±0,67	20,75±0,52	I4,56±0,37	9,44 ±0,24	7,65±0,28	5,52±0,22	4,74±0,I5	4,06±0,I3
2,7	30,9I±0,86	29,39±0,82	24,90±0,70	I9,22±0,54	I3,33±0,38	7,98±0,23	6,77±0,27	4,80±0,I9	4,I2±0,I4	3,46±0,I2
2,9	28,7I±0,45	27,48±0,43	22,69±0,37	I7,44±0,28	I2,I7±0,20	7,7I±0,I3	5,87±0,I9	4,I0±0,I3	3,50±0,08	2,97±0,07
3,I	26,60±0,26	25,68±0,25	2I,I0±0,2I	I5,86±0,I5	II,08±0,I3	6,92±0,08	5,I2±0,I4	3,54±0,I0	2,99±0,06	2,53±0,04
3,3	24,53±0,I6	23,88±0,I6	I9,53±0,I5	I4,36±0,II	I0,05±0,09	6,23±0,06	4,46±0,II	3,03±0,08	2,56±0,04	2,I6±0,03
3,5	22,42±0,I6	22,02±0,I6	I7,98±0,I3	I3,06±0,09	9,05 ±0,09	5,60±0,06	3,88±0,08	2,63±0,06	2,I9±0,03	I,85±0,02
3,7	20,46±0,I8	20,30±0,I9	I6,38±0,I5	II,8I±0,II	8,I9 ±0,I0	5,02±0,06	3,37±0,07	2,26±0,05	I,87±0,03	I,58±0,02
3,9	I8,62±0,I9	I8,70±0,I9	I4,92±0,I4	I0,65±0,I0	7,38±0,09	4,49±0,06	2,94±0,06	I,96±0,04	I,60±0,03	I,34±0,02
4,I	I6,8I±0,23	I7,I0±0,24	I3,56±0,I9	9,57 ±0,I3	6,6I±0,I9	4,0I±0,07	2,55±0,06	I,68±0,04	I,36±0,03	I,I5±0,02
4,3	I5,I7±0,24	I5,50±0,24	I2,26±0,I9	8,58 ±0,I3	5,93±0,I3	3,58±0,07	2,2I±0,06	I,45±0,03	I,I7∓0,03	0,98±0,02
4,5	I3,80±0,25	I4,00±0,26	II,06±0,20	7,68±0,I4	5,32±0,II	3,I8±0,07	I,92±0,06	I,26±0,03	I,00±0,03	0,84±0,02
4,7	I2,48±0,24	I2,70±0,24	9,93 ±0,I9	6,86±0,I3	4,75±0,II	2,84±0,06	I,67±0,06	I,09±0,03	0,86±0,03	0,72±0,02
4,9	II,I8±0,23	II,44±0,24	8,9I±0,I9	6,I0±0,I3	4,24±0,I0	2,5I±0,06	I,45±0,06	0,96±0,03	0,73±0,03	0,6I±0,02
5,I	9,98±0,20	I0,24±0,2I	7,99±0,I6	5,4I±0,II	3,8I±0,09	2,23±0,06	I,26±0,06	0,82±0,03	0,62±0,03	0,53±0,02
5.3	8,90±0,I6	9,20±0,I7	7,I6±0,I4	4,82±0,09	3,40±0,08	I,98±0,06	I,I0±0,06	0,7I±0,03	0,54±0,03	0,38±0,02
5,5	7,94±0,I6	8,24±0,I7	6,4I±0,I3	4,24±0,09	3,02±0,07	I,76±0,04	0,96±0,06	0,62±0,03	0,45±0,02	0,32±0,02
5,7	7,06±0,I7	7,34±0,I7	5,38±0,I4	3,76±0,09	2,69±0,08	I,54±0,04	0,82±0,06	0,53±0,03	0,39±0,02	0,28±0,02
5,9	6,28±0,I0	6,58±0,I0	5,09±0,08	3,36±0,06	2,42±0,06	I,40±0,03	0,73±0,06	0,47±0,03	0,35±0,02	0,24±0,02
6,I	5,57±0,I0	5,80±0,II	4,45±0,09	2,96±0,06	2,I4±0,06	I,20±0,03	0,62±0,04	0,4I±0,02	0,28±0,02	0,2I±0,02
6,3	4,90±0,I0	5,II±0,I0	3,94±0,08	2,60±0,06	I,9I±0,06	I,08±0,03	0,55±0,04	0,35±0,02	0,25±0,02	0,I7±0,0I
6,5	4,38±0,08	4,55±0,08	3,48±0,07	2,30±0,04	I,70±0,06	0,96±0,03	0,47±0,04	0,30±0,02	0,2I±0,02	0,I5±0,0I
6,7	3,86±0,09	4,06±0,I0	3,08±0,09	2,04±0,06	I,52±0,06	0,86±0,03	0,40±0,03	0,26±0,02	0,I8±0,0I	0,I3±0,0I
6,9	3,42±0,06	3,58±0,06	2,76±0,04	I,80±0,03	I,35±0,04	0,76±0,02	0,36±0,03	0,23±0,02	0,I5±0,0I	0,I2±0,0I
7,I	3,02±0,06	3,I6±0,06	2,43± 0,04	I,58±0,03	I,20±0,03	0,67±0,02	0,3I±0,03	0,20±0,02	0,I4±0,0I	0,I0±0,0I
7,3	2,66±0,06	2,77±0,06	2,I5±0,04	I,39±0,03	I,06±0,03	0,59±0,02	0,27±0,03	0,I8±0,02	0,I2±0,0I	0,08±0,0I
7,5	2,36±0,06	2,44±0,06	I,89±0,04	I,23±0,03	0,95±0,03	0,53±0,02	0,23±0,03	0,I5±0,0I	0,I0±0,0I	0,07±0,0I
7,7	2,08±0,06	2,I5±0,06	I,66±0,03	I,08±0,02	0,84±0,03	0,47±0,02	0,2I±0,03	0,I3±0,0I	0,09±0,0I	0,06±0,0I
7,9	I,84±0,04	I,89±0,06	I,47±0,04	0,95±0,02	0,75±0,03	0,4I±0,02	0,I8±0,02	0,I2±0,0I	0,07±0,0I	0,06±0,0I
8,I	I,62±0,04	I,66±0,04	I,28±0,03	0,83±0,02	0,67±0,02	0,36±0,0I	0,I5±0,02	0,I0±0,0I	0,06±0,0I	0,04±0,0I

Note: All data are multiplied by 100.

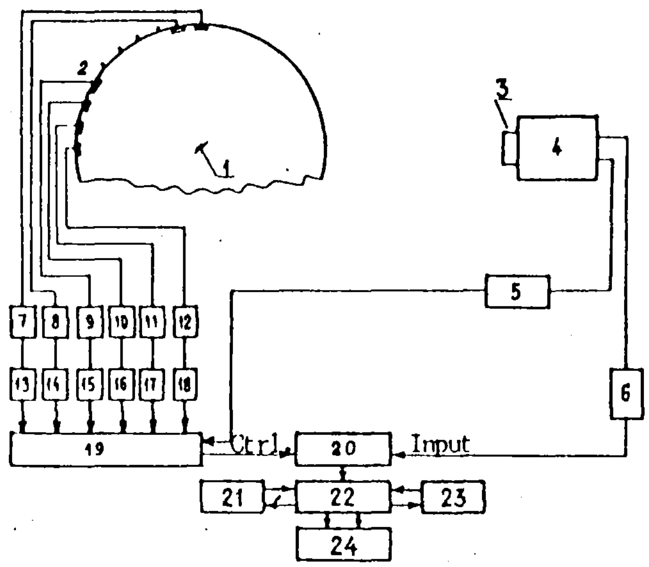

Figure 1. Block diagram of the experiment: (1) ^{252}Cf layer; (2) semiconductor detectors; (3) stilbene; (4) photomultiplier; (5) separation circuit; (6-12) spectrometer amplifiers; (13-18) integral discriminators; (19) detector number encoder; (20) analog-to-digital converter; (21) external memory; (22) PMC magnetic operating store; (23) tape recorder; (24) computer.

of the apparatus over the whole series of measurements was adequate at $\pm$ 0.2%.

2. The amplitude distribution of the Compton recoil electrons from γ-quanta produced by ^{137}Cs was measured using the (n-γ) separation circuit in order to monitor its function. γ-quanta from ^{137}Cs were suppressed, as a rule, by factors of 500 or more.

3. The discrimination level and degree of amplification in the fragment channels were monitored from the amplitude distribution of the fission fragments. These spectrometric channels were very stable in their operation, and for this reason no corrections were required during the experiment.

4. To reduce all the measurement channels to the same solid angle of fragment detection, the number of fission fragments detected by each semiconductor counter per unit time was measured. The differences in the solid angles of fission fragment detection did not exceed $\pm$ 3%.

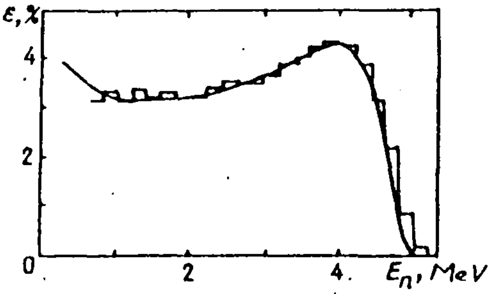

Figure 2. Recoil proton distribution for E_n = 4.7 MeV. Solid line: experiment; histogram: calculation.

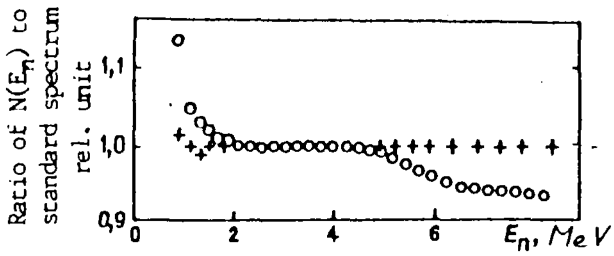

Figure 3. The integral ^{252}Cf fission neutron spectrum as a ratio of the standard ^{252}Cf fission neutron spectrum. Reconstruction result: o - with calculated response function; + - after correcting spectrometer response function.

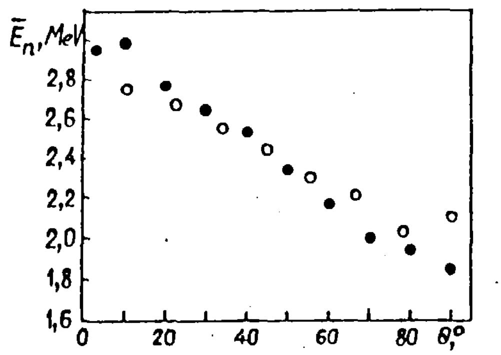

Figure 4. Angular distribution of ^{252}Cf spontaneous fission neutrons. Data: • - present work; O - [1]. Errors are commensurate with the sizes of the conventional symbols.

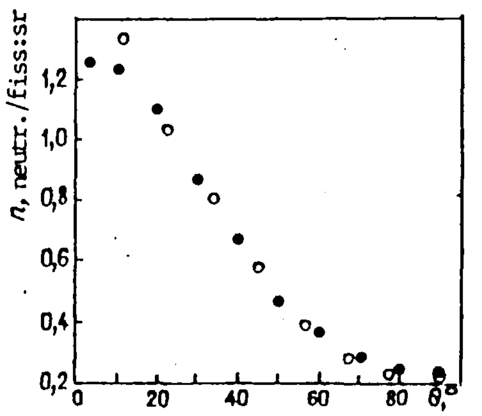

Figure 5. Dependence of intermediate spectrum energies on neutron emission angle in the laboratory system. Data: • - present work; O - [1]. Errors are commensurate with the dimensions of the conventional symbols.

5. The integral spectrum for ^{252}Cf spontaneous fission neutrons was measured in a coincidence arrangement with the fission fragments recorded by a semiconductor counter 0.5 mm from the surface of the layer. In this way, approximately 95% of all the fragments produced in the target were recorded. Then, with exactly the same geometry, the scattered neutron background was measured using the shadow cone. The integral spectrum obtained was subsequently used to correct the calculated response function of the neutron detector assuming the measured ^{252}Cf fission neutron spectrum to be standard.

In order to exclude the possibility that any of the channels for measuring the neutron spectra at various angles to the axis of fragment separation might not be identical, each measurement cycle was begun by shifting the fragment detectors and their corresponding spectrometer channels to other angles. The final neutron amplitude distribution obtained by the apparatus for each angle was arrived at by summing the six spectra obtained using each of the spectrometer channels available. This being the case, the total number of fragments recorded by each semiconductor detector was 2.43×10^7 fissions. From these measurements, 24 sets of experimental data were stored on magnetic tape, containing neutron spectrum information and also information on the calibration spectra and constants required for subsequent processing.

In addition to the experiment described, we conducted an additional test on a Van de Graaff electrostatic accelerator in order to determine absolutely the luminous output of the stilbene crystal used. This was carried out using mono-energetic neutrons from the $T(p,n)^4He$ and $D(p,n)^3He$ reactions. The correspondence between the energies of the electrons and protons giving rise to various pulse amplitudes was determined. Measurements were carried out for two targets on mono-energetic neutrons at energies of 0.5, 0.7, 0.9, 1.1 and 1.3 MeV and 3.5, 4.0, 4.5, 4.7 and 4.9 MeV. It proved to be the case that the link between light output and recoil proton energy was well described by Birks' semi-empirical formula:

$$\frac{dP}{dE} = 1\Big/\left(1 + kB\frac{dE}{dx}\right),$$

where P is a value directly proportional to the luminous output of the crystal, kB = 0.012 $mg \cdot cm^{-2} MeV^{-1}$ and x is the path length of the particle in the crystal. Using this formula and the tables shown in Ref. [5], the luminous output of the crystal as a function of recoil proton energy was calculated in the range 0.2–8 MeV in steps of 0.2 MeV. The function obtained was subsequently used to obtain recoil proton spectra from the distributions provided by the apparatus.

Processing of data and measurement results

The procedure for processing the data obtained in the experiment included the following stages: (1) correction for the slight spread in the solid angles of fragment detection; (2) conversion, using the pooling method, of the distributions obtained from the apparatus into recoil proton distributions; (3) subtraction of the scattered neutron backgrounds. The fourth and final stage in the processing consisted of reconstructing the neutron spectra from the recoil proton distributions obtained from the apparatus. The simplest and most widely used method for reconstructing neutron spectra is the differentiation method [6]. However, this provides satisfactory results only if a sufficiently thin crystal is used and if the recoil proton spectrum can be measured with a high degree of statistical accuracy. Strictly speaking, neither of these conditions were met in our case. For this reason a new method of reconstruction was developed using a priori fission neutron spectrum information. The fission neutron spectra are described by superposing Γ-distributions of the form:

$$\Phi(E_n) = \sum_k A_k E_n^{\alpha} \exp(-\beta_k E_n), \qquad (1)$$

where E_n is the neutron energy, A^k are coefficients, index k has the values 1, 2, ..., 20 and the value of $1/\beta_k$ = 0.1, 0.3, ..., 3.9 MeV. The applicability of this type of algorithm in reconstructing fission neutron spectra and its comparison with the results obtained by reconstruction using the differentiation and statistical regularization methods is examined in Refs [7] and [8]. It was demonstrated that the method developed avoids the oscillations found in the differentiation method and makes it possible to calculate a realistic spectrometer response function; it also reproduces results well at relatively low levels of statistical accuracy in the measurement of the recoil proton spectra.

It is known that the relationship between the fission spectrum $\Phi(E_n)$ and the recoil proton spectrum $N(E_p)$ obtained by the apparatus is expressed by a Fredholm equation of the first kind:

$$N(E_p) = \int_{E_p}^{E_{max}} \Phi(E_n) G(E_n, E_p) dE_n \,, \tag{2}$$

where the kernel of the equation $G(E_n,E_p)$ is the spectrometer response function. By inserting expression (1) into equation (2) and by replacing the integration with a summation, we obtain:

$$N(E_p) = \sum_n \sum_k A_k G(E_p, E_n) E_n^{\alpha} exp(-\beta_k E_n) \,. \tag{3}$$

The system of equations was used to determine the coefficients A_k. To implement the algorithm on the computer, the method of least directional divergence was chosen [9]. The search procedure used for the A_k coefficient was iterative:

$$A_k^{(w)} = A_k^{(w-1)} \left(\sum_{i=1}^{n} B_{ik} \frac{N_i}{F_i^{(w)}} \right) \Big/ \sum_{i=1}^{n} B_{ik} \quad ,$$

where $B_{ik} = \sum_{j=i}^{n} G_{jk} E_j^{\alpha} exp(-\beta_k E_j)$, N_i is the experimental recoil proton spectrum and $F_i^{(w)} = \sum_{k=1}^{m} B_{ik} A_k^{(w)}$ — is the calculated recoil proton spectrum. The initial approximation for the A_k coefficients was uniform, and in fact $A_k^0 = 1$.

A realistic spectrometer response function G_{ik} was calculated using a Monte Carlo method in accordance with the program in Ref. [10]. To achieve a better agreement between calculation and experiment, the following input data were used in this program: the relationship of luminous output to recoil proton energy was taken from Ref. [5]; the relationship of luminous output to the angle between the crystal axis and the direction of the recoil proton pulse was represented by the expression $C(\xi) = 0.176\ (1-3.111\ \sin^4\xi)^{-1/2}$; the function used for the relationship of the degree of resolution of the spectrometer to energy had the form $\sigma(E) = 0.09 \times E^{0.5}$. Fig. 2 shows the amplitude distribution of the recoil protons for a neutron energy of 4.7 MeV. It is evident that the agreement between the experimental and the calculated distribution is satisfactory.

The integral ^{252}Cf fission neutron spectrum reconstructed using this method is shown in Fig. 3 as a ratio of the standard ^{252}Cf fission neutron spectrum taken from the ENDF/B-V library version. It should be noted that around the threshold level and at neutron energies of over 6 MeV, there are deviations between the integral spectrum and the standard, which may be caused either by inaccuracy in the response function calculations or by unknown systematic errors. To remove this uncertainty, the spectrometer response function was corrected and the standard form of the integral ^{252}Cf fission neutron spectrum was obtained.

The energy distributions for the ten angles measured in the energy range 0.7-8.1 MeV were reconstructed using this method and taking into account the corrected spectrometer response function. The table contains digital data for the differential energy spectra of fission neutrons $n(E_n,\theta_\lambda)$ as a function of angle of emission in the laboratory system, and the measurement and spectrum reconstruction errors are shown.

Discussion of results

The integral neutron spectrum obtained by summation of the differential spectra in accordance with the expression $N(E_n)=2\pi\sum n(E_n,\theta_\lambda)\sin\theta_\lambda\Delta\theta_\lambda$ agrees with the standard form of the ^{252}Cf spontaneous fission neutron spectrum to within ± 2% and is well described by a Maxwellian distribution with parameters T = 1.42 MeV and $\bar{\nu}$ = 3.756 neutr./fiss. This is evidence of the reliability of the experimental data.

Figures 4 and 5 show the number of neutrons and mean spectral energies as functions of the angle of emission in the laboratory system used in Ref. [1], reduced to the same energy range as the data in the present work. On the whole, the angular distributions agree fairly well; however, the point corresponding to an angle of 11.25° is higher than in our data by approximately 7%. For intermediate energies, agreement is quite good for angles from 30° to 60°. In the small angle region, the spectra are harder than given in Ref. [1], and significantly softer at larger angles. The same divergence between the intermediate energies of the differential spectra from Ref. [1] and their own data was noted by the authors of Ref. [2].

Figure 6 shows the neutron energy distributions obtained by converting the distributions $\rho(v_n\theta\lambda)$ from Ref. [1] to the form $n(E_n,\theta_\lambda)$. The spectra obtained in the present work and in Ref. [1] clearly differ most significantly for angles close to 10° and 90°. One of the reasons for these divergences may be the distorting effect of the scattered neutron background on the results in Ref. [1], since for comparable solid angles of neutron detection the volume of the detector used in Ref. [1] was 25 times that of our stilbene crystal, and consequently the sensitivity of the method used in Ref. [1] to the background was at least of order of magnitude higher than the sensitivity of the method used here.

A detailed comparison of the results of the present work with those of Ref. [2] could not be made, as only the zeroth and first moments of distribution are given in the latter work and there is no information on the

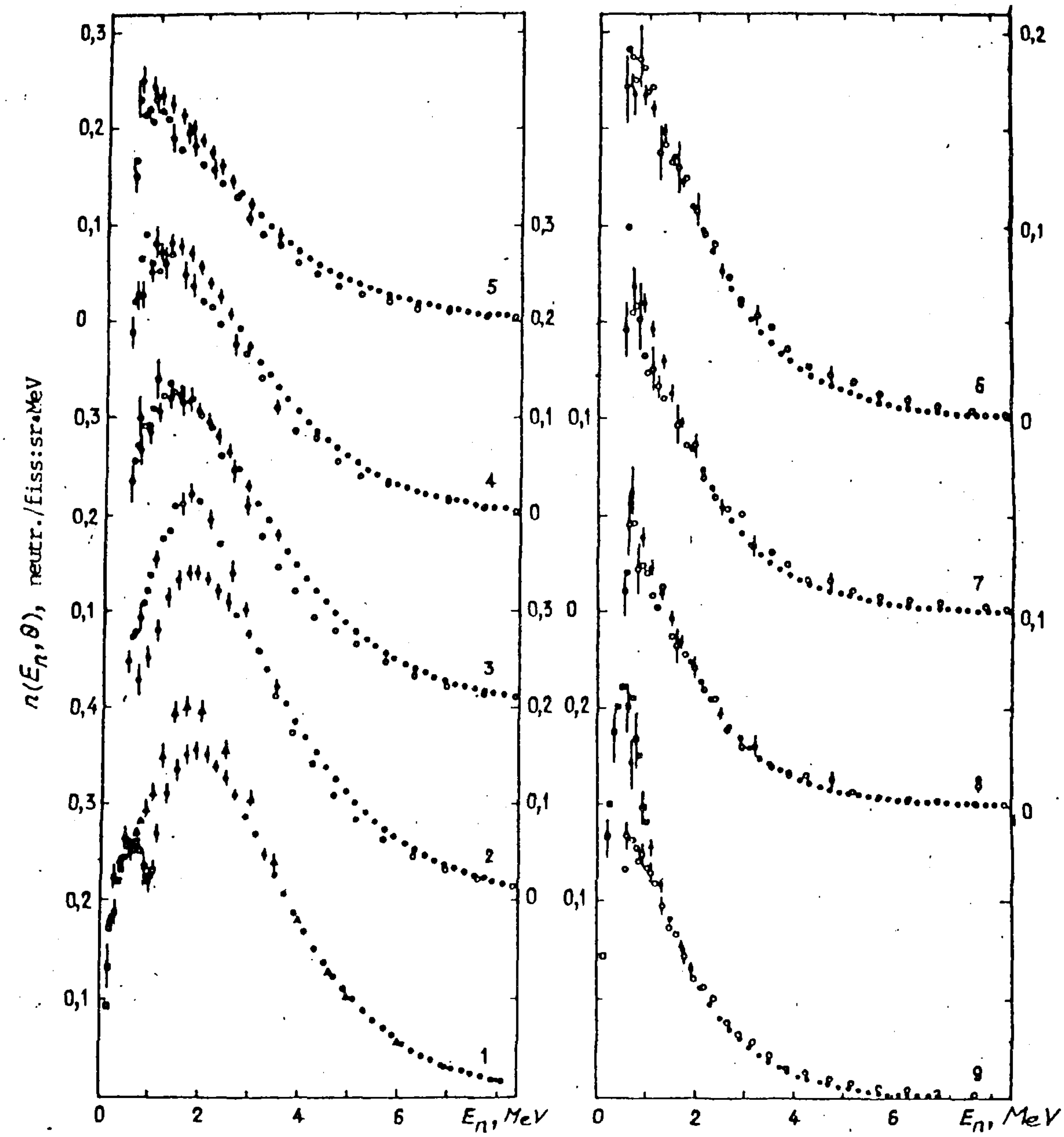

Figure 6. The energy spectra of spontaneous ^{252}Cf fission neutrons. Experimental data: ● - present work; o - [1], obtained by converting the distributions $\rho(v_n, \theta_\lambda)$ into the form $n(E_n, \theta_л)$; Δ - [2]; □ - [11]; 1) ● - 3°, □ - 3°, Δ - 4°; 2) ● - 10°, o - 11,25°; 3) ● - 20°, o - 22,5°; 4) ● - 30°, o - 33,75°; 5) ● - 40°, o - 45°; 6) ● - 60°, o - 56,25°; 7) ● - 70°, o - 67,5°; 8) ● - 80°, o - 78,75°; 9) ● - 90°, o - 90°

neutron energy spectra for most of the angles (except 4°). The neutron energy spectrum for 4° taken from Ref. [2] is denoted in Fig. 6 by the symbol Δ. It can be seen that the neutron yield in the energy range 1-3 MeV according to Ref. [2] is approximately 10-15% higher than according to our data. It is difficult to identify the reason for this divergence, because the experimental method used in Ref. [2] is described in a very condensed form, and it is not clear, for example, how the scattered neutron background was measured and taken into account.

Figure 6 shows the neutron spectrum measurements taken from Ref. [11] for angles 3° and 90° in the energy range 0.1-1 MeV. These data are in good agreement with the results of our experiment and in part supplement it. The irregularity found in the 3° energy distribution in the range 0.7-1 MeV is striking. According to the evaporation theory, it is precisely in this range where the neutron energy coincides with the mean kinetic energy of the fragments pertaining to one nucleon, that a minimum must be observed in the energy distribution pattern for an angle close to 0°.

It can thus be seen that the results obtained in our work indicate that the picture of the angular and energy distributions of prompt neutrons from spontaneous ^{252}Cf fission is somewhat different from that established in Ref. [1]. This particularly concerns angles between the direction of emission of fragments and of neutrons of around 0° and 90°. Thus, the disagreement for the energy range 1 MeV $\lesssim E_n \lesssim$ 3 MeV where $\theta_\lambda \approx$ 10% is 15-20%. For angles around 90°, the maximum disagreement is observed in the energy range up to 1.5 MeV and also amounts to 15-20%. Taking into account the significantly greater sensitivity to the scattered neutron background of the method used in Ref. [1], and also the nature of the divergences observed, the reason for the latter can be assumed to be inadequate allowance in Ref. [1] for the scattered neutron background. However, strictly speaking, this is only an assumption and further research is required in order to establish the true picture of the angular and energy distributions of prompt neutrons from the spontaneous fission of ^{252}Cf.

REFERENCES

[1] BOWMAN, H.R., THOMPSON, S.L., MILTON, J.C., SWIATECKI, W.J., Phys. Rev. 126 6 (1962) 2120.

[2] BATENKOV, O.I., BLINOV, M.V., VITENKO, V.A., Physics and Chemistry of Fission (Proc. Symp. Jülich, 14-18 May 1979), Vol. II, IAEA, Vienna (1980) 267.

[3] D'YACHENKO, P.P., SEREGINA, E.A., Official Bulletin of the USSR State Committee on Inventions and Discoveries 44 (1980) 299. [In Russian].

[4] SUBBAH, B., SUHAMI, A., Nucl. Instrum. Methods 58 (1968) 102.

[5] SWARTZ, K., OWEN, G., in Fizika bystrykh nejtronov, Atomizdat, Moscow (1963), Vol. I, p. 231, translated from Russian.

SWARTZ, C.D., OWEN, G.E., "Recoil detection in scintillators", Fast Neutron Physics (MARIOM, J.B., FOWLER, J.L., Eds), Vol. I, New York, NY, (1960-63) 211, 246.

[6] DULIN, V.A., KAZANSKIJ, Yu.A., KUZNETSOV, V.F., SMIRENKIN, G.N., Pribori i tekhnika ehksperimenta 2 (1961) 35.

[7] D'YACHENKO, P.P., SEREGINA, E.A., TARASKO, M.Z., Voprosy atomnoj nauki i tekhniki, Ser. Yadernye konstanty, 2 41 (1981) 18.

[8] SEREGINA, E.A., D'YACHENKO, P.P., DUSHIN, V.N., in Nejtronnaya fizika (Proc. 6th All-Union Conf. on Neutron Physics, Kiev, 2-6 Oct. 1983), Vol. 4, TsNIIatominform, Moscow (1984) 350.

[9] TARASKO, M.Z., Preprint FEhI-1446, Obninsk (1983) [in Russian].

[10] CHULKOV, L.V., Preprint IAEh-2594, Moscow (1974) [in Russian].

[11] PIKSAJKIN, V.M., D'YACHENKO, P.P., LAJTAI, A. et al., Yadernaya fizika 25 3 (1977) 495.

Article submitted 6 July 1984